

**EVALUATION OF GAS IN PLACE, DRAINAGE EFFICIENCY
AND PRODUCTION OPTIMIZATION AT "X" GAS FIELD**

THESIS

**Submitted in partial fulfillment of the requirements for
MASTER OF ENGINEERING DEGREE
at the Department of Petroleum Engineering**

By

NUGROHO MARSIYANTO

NIM: 22211029

(Petroleum Engineering Program)



**DEPARTMENT OF PETROLEUM ENGINEERING
FACULTY OF MINING AND PETROLEUM ENGINEERING
INSTITUTE OF TECHNOLOGY BANDUNG**

2014

**EVALUATION OF GAS IN PLACE, DRAINAGE EFFICIENCY
AND PRODUCTION OPTIMIZATION AT "X" GAS FIELD**

By
Nugroho Marsiyanto
NIM: 22211029
(Petroleum Engineering Program)

Submitted in partial fulfillment of the requirements for
MASTER OF ENGINEERING DEGREE
at the Department of Petroleum Engineering
Faculty of Mining and Petroleum Engineering
Institute Of Technology Bandung

Approved by Advisor

Bandung, March 2014



Dr. Ir. Sudjati Rachmat, DEA
NIP. 195509021980031005

ABSTRACT

EVALUATION OF GAS IN PLACE, DRAINAGE EFFICIENCY AND PRODUCTION OPTIMIZATION AT "X" GAS FIELD

By

Nugroho Marsiyanto

NIM: 22211029

(Study Program of Petroleum Engineering)

An exploration or exploitation gas field always has a question about amount of hydrocarbon which can be produced at surface and how much the reserve can be covered optimally. This recovered reserve (gas) number is needed for investment & economic calculation and how to optimize the production by implementing good reservoir management.

In gas reservoir both production and pressure history data are very important for implementation of good reservoir management. After field and wells have been produced for long enough, those 2 kind data can control and determine the work plan for production optimization. "X" gas field has been producing since 2002, so production and reservoir pressure data have been recorded routinely. By evaluating production and reservoir pressure data, re-work in estimation of IGIP, evaluate upside potential to determine drainage area and production optimization are assessed. Material Balance and Decline Curve methods are applied to evaluate this job. The MBE model is built to see IGIP by wells and field. It will be also compared with DC method and result from previous study. Lowering intake suction pressure of compressor is decided to add more reserve and drain the gas in reservoir until very low abandonment pressure.

From this study, IGIP is estimated about 81 BSCF, no infill well development is needed and lowering intake suction pressure of compressor to 50 psia is recommended for additional RF 6% of IGIP.

(Keywords: IGIP, Material Balance, Decline Curve, Drainage Area, Compressor suction pressure)

ABSTRAK

EVALUASI GAS *IN PLACE*, EFFISIENSI AREAL PENGURASAN DAN OPTIMASI PRODUKSI DI LAPANGAN GAS "X"

Oleh

Nugroho Marsiyanto

NIM: 22211029

(Program Studi Teknik Perminyakan)

Aktifitas eksplorasi dan produksi lapangan gas selalu memberikan pertanyaan jumlah hidrokarbon yang akan diproduksi di permukaan dan berapa banyak cadangan yang akan diperoleh secara optimal. Jumlah cadangan hidrokarbon (gas) ini diperlukan untuk perhitungan biaya investasi dan keekonomian proyek serta bagaimana mengoptimalkan produksinya dengan cara penerapan pengelolaan reservoir yang baik.

Di pengelolalan lapangan gas, sejarah data produksi dan tekanan reservoir sangat penting untuk pelaksanaan pengelolaan reservoir yang baik. Setelah lapangan dan sumur-sumur diproduksi dalam waktu yang cukup lama, kedua data tersebut dapat digunakan untuk mengontrol dan menentukan arah rencana kerja untuk optimisasi produksi. Lapangan gas "X" telah berproduksi sejak tahun 2002, sehingga sejarah data produksi dan tekanan reservoir telah dicatat secara rutin. Dengan mengevaluasi data produksi dan reservoirnya, perhitungan ulang utk *IGIP*, evaluasi potensi untuk menentukan areal pengurasan dan optimasi produksi dilakukan. *Metoda Material Balance* dan *Decline Curve* digunakan untuk mengevaluasi pekerjaan-pekerjaan tersebut. Model *Material Balance* dibuat untuk menghitung *IGIP* baik tiap well dan lapangan. Hasilnya akan juga dibandingkan dengan perhitungan *IGIP* dengan menggunakan metoda *Decline Curve* serta dengan metoda-metoda lain untuk perhitungan *IGIP*-nya dari studi sebelumnya. Proyek penurunan tekanan hisap kompressor akan dilakukan untuk menambah perolehan cadangan dan menguras gas di dalam reservoir hingga tekanan reservoir mencapai tekanan paling rendah untuk ditinggalkan.

Dari hasil studi ini, *IGIP* diperkirakan sekitar 81 BSCF, tidak diperlukannya tambahan sumur pengembangan untuk pengurasan dan penurunan tekanan hisap compressor ke 50 psia direkomendasikan untuk memberikan perolehan tambahan cadangan gas sekitar 6% dari *IGIP*-nya.

(Kata-kata kunci : *IGIP*, *Material balance*, *Decline Curve*, Areal Pengurasan, Tekanan hisap Kompresor)

THE DIRECTIVE OF THESIS USING

This Master Degree thesis is listed and available at Institute Of Technology Bandung and open for anyone who utilizes this thesis as reference. All right reserved refers to HaKI. Quote and summary taken from this thesis only can be done with permission from the writer and be noted as the source.

No parts of this thesis may be reproduced or distributed in any forms or by any means, without permission in writing from Director of Master Program of Institute Of Technology Bandung.

DEDICATION

This thesis is dedicated to my father & my mother who always taught me knowledge ranging from children to the present. It is also dedicated to my wife and our children who always support and pray for our family.

ACKNOWLEDGMENTS

Praise and thanks to Allah SWT, who has always given the writer the blessing and strength to finish this thesis of Master Degree with title "Evaluation of Gas In Place, Drainage Efficiency and Production Optimization at X Gas Field".

This thesis is one of requirements to obtain Master Degree at Institute of Technology Bandung. The writer really expresses my sincerest gratitude to the persons who help and support directly and indirectly to complete this thesis as mentioned below:

1. Dr. Ir. Sudjati Rachmat, DEA, as advisor for his guidance and advice to complete this thesis.
2. Dr. Ir. Taufan Marhaendrajana, M.Sc. as Principal of Petroleum Engineering Study Program at ITB
3. Prof. Dr. Ir. Pudjo Sukarno, MSc and Dr. Ir Sutopo as the examiner who give their time to evaluate this thesis.
4. All lectures and Staffs at Master Degree of Petroleum Engineering Study Program at ITB
5. All of classmates at Master Degree of Petroleum Engineering Study Program at ITB period 2011.
6. All of them who I can't mention one by one for their direct and indirect support to make me finish this thesis and complete my master degree in petroleum engineering at ITB.

Finally, the writer realizes that this thesis is far from being perfect; therefore, any criticism for the improvement of this thesis will be pleasantly accepted and the writer hopes that this thesis will be useful for the readers.

Bandung, March 2014

Nugroho Marsiyanto
The writer

CONTENTS

ABSTRACT	ii
ABSTRAK	iii
THE DIRECTIVE OF THESIS USING	v
DEDICATION	vi
ACKNOWLEDGMENTS	vii
CONTENTS	viii
LIST OF ATTACHMENTS	x
LIST OF FIGURES	xi
LIST OF TABLES	xii
LIST OF ABBREVIATIONS AND SYMBOLS	xiii
CHAPTER I INTRODUCTION	1
I.1 Background	1
I.2 Purpose	1
I.3 Scope of Work	2
I.4 Data and Methodology	2
I.5 Thesis Outline	2
CHAPTER II SUPPORTED THEORIES	4
II.1 Gas Reservoir	4
II.2 Gas Fluid Properties	5
II.2.1 Gas Volume Formation Factor.....	5
II.2.2 Gas Viscosity.....	5
II.2.3 Gas Compressibility Factor (z)	6
II.3 Well Deliverability	7
II.4 Initial Gas In Place Method	7
II.4.1 Material Balance Method.....	7

II.4.2	Decline Curve Method.....	8
CHAPTER III GEOLOGICAL & RESERVOIR CHARACTERIZATION.....		11
III.1	Geology & Stratigraphy	11
III.1.1	Regional Geology	11
III.1.2	Stratigraphy	14
III.2	Reservoir Characterization	20
III.2.1	Reservoir Fluid Properties Analysis.....	20
III.2.2	Core Rutin Analysis.....	21
III.2.3	Log Interpretation	22
CHAPTER IV DATA CALCULATION AND ANALYSIS.....		23
IV.1	Data Calculation	23
IV.1.1	Reservoir Pressure And Temperature.....	23
IV.1.2	Reservoir <i>Cut-Off</i>	24
IV.1.3	Production Performance & Well Deliverability.....	25
IV.2	Analysis	26
IV.2.1	Reservoir Type	26
IV.2.2	Material Balance Method.....	27
IV.2.3	Decline Curve Method.....	31
IV.2.4	Results Based On Methods	32
IV.3	Drainage Area	34
IV.4	Production Optimization & Surface Facility Capability.....	35
IV.4.1	Well & Field Production Deliverability & Optimization.....	35
IV.4.2	Surface Facility Capability.....	36
IV.4.2.1	Pipeline & manifold	36
IV.4.2.2	Slug Catcher And Gas Liquid Separator	37
IV.4.2.3	Compressor	38
CHAPTER V CONCLUSION AND FUTURE WORK.....		40
V.1	Conclusion.....	40
V.2	Future Work	41
REFERENCES.....		42

LIST OF ATTACHMENTS

Attachment 1 PVT study of samples from the MDL-1.....	43
Attachment 2 PVT study of samples from the MDL-2.....	44
Attachment 3 PVT study of samples from the MDL-3.....	45
Attachment 4 “X” gas field BRF structure map.....	46
Attachment 5 Permeability and porosity data at corresponding depths.....	47
Attachment 6 Summary of log interpretation result.....	48
Attachment 7 “X” gas field pressure history record	49
Attachment 8 Production and reservoir pressure history Mdl-01	50
Attachment 9 Production and reservoir pressure history Mdl-02	51
Attachment 10 Production and reservoir pressure history Mdl-03	52
Attachment 11 Well diagram Mdl-01	53
Attachment 12 Well diagram Mdl-02	54
Attachment 13 Well diagram Mdl-03	55
Attachment 14 IGIP Mdl-01 based on MBE model	56
Attachment 15 IGIP Mdl-02 based on MBE model	57
Attachment 16 IGIP Mdl-03 based on MBE model	58
Attachment 17 IGIP Mdl-01 based on DC analysis.....	59
Attachment 18 IGIP Mdl-02 based on DC analysis.....	60
Attachment 19 IGIP Mdl-03 based on DC analysis.....	61
Attachment 20 Schematic wells and surface facilities “X” gas field.....	62

LIST OF FIGURES

Figure 2-1 Typical gas reservoir phase diagram (James F. Lea 2008)	4
Figure 2-2 Compressibility factors for a natural gas as a function of pressure at constant temperature (Smith, 1990)	6
Figure 2-3 Pressure – production curve for a gas field on Cartesian coordinates (Smith, 1990)	8
Figure 2-4 Decline curve rate / time (exponential, harmonic, hyperbolic) (Ahmed, 2006)	10
Figure 3-1 Location map of “X” gas field	12
Figure 3-2 General stratigraphic of “X” gas field	19
Figure 3-3 Typical log of “X” gas wells	20
Figure 3-4 Plot of pressure vs compressibility factor	21
Figure 3-5 Plot of permeability versus porosity	22
Figure 4-1 Reservoir pressure of “X” gas field vs. time	23
Figure 4-2 Reservoir temperature of “X” gas field versus time	24
Figure 4-3 Production and reservoir pressure history of “X” gas field	25
Figure 4-4 PVT laboratory result and production data that determines “X” gas field as dry gas reservoir	27
Figure 4-5 Fluid properties data to generate MBAL model	28
Figure 4-6 Gas deviation factor (Z) of “X” gas reservoir refer to MBAL model	28
Figure 4-7 History match of reservoir pressure, simulation and prediction	29
Figure 4-8 Straightline MBE method for IGIP “X” gas field	30
Figure 4-9 Dominant drive of “X” gas field	31
Figure 4-10 Decline curve method of “X” gas field	32
Figure 4-11 Drainage area of “X” gas field in time structure map	34

LIST OF TABLES

Table 4-1 IGIP MBal analysis by well and IGIP Decline Curve by well.....	33
Table 4-2 Gas liquid separator design basis.....	37
Table 4-3 Compressor specification with suction pressure 550 psia	38
Table 4-4 Compressor specification with suction pressure 200 psia	38

LIST OF ABBREVIATIONS AND SYMBOLS

b	Arps' decline curve exponent (Exponential $b=0$, Hyperbolic $0 < b < 1$, Harmonic $b=1$)
B _g	Gas formation volume factor, ft ³ /scf
BRF	Batu Raja Formation
BSCF	Billion Standard Cubic Feet
DC	Decline Curve
D _i	Initial decline rate, day ⁻¹
IGIP	Initial Gas In Place
Mbal	Material Balance
MBE	Material Balance Equation
MMSCFD	Million Standard Cubic Feet Per Day
MSCFD	Thousand Standard Cubic Feet Per Day
P _c	Critical Pressure
Psia	Pounds square inch
PVT	Pore Volume Temperature
q _i	Initial gas flow rate, MMscf/day
q _t	Gas flow rate at time t, MMscf/day
t	Time, days
TAF	Talang Akar Formation
T _c	Critical Temperature
V _c	Critical Volume
V _{p,T}	Volume of gas at pressure p and temperature, T, ft ³
V _{sc}	Volume of gas at standard conditions, scf
Z	Gas deviation factor
μ _g	Gas viscosity, centipoise

CHAPTER I INTRODUCTION

I.1 Background

After exploration or delineation drilling is completed and find the accumulation of hydrocarbon, the next step is to predict initial hydrocarbon (gas) in place in the reservoir, reservoir productivity and performance. The most important factor in developing and planning of gas production from a productive reservoir is estimation of initial gas in place and recovery factor (reserve).

The method to estimate IGIP, drainage efficiency and production optimization in gas reservoir have been developed in periodically. This estimation must be calculated periodically to get the accurate number. In the early stage of gas field development when there is no production data yet, the volumetric method is used to estimate IGIP. In this stage, the most used data is geological data. After couple development wells have been drilled and produced, the material balance, decline curve and simulation reservoir are methods used to estimate IGIP and reserve.

By production time of the gas field from development wells in longer production period, the performance prediction of reservoir will be more accurate. Through reservoir performance study, the drainage efficiency of the production wells can be predicted whether the existing wells can produce optimal and efficient to drain the reserve or may need more activities to improve the production through new infill wells drilling, workover or wellservice activities and surface facilities optimization.

I.2 Purpose

The purpose of this study is to estimate IGIP, evaluate reservoir performance to optimize the production through wells activities & surface facilities optimization and evaluate the drainage efficiency from the current existing wells.

I.3 Scope of Work

The “X” gas field is categorized as a dry gas reservoir therefore for this study will focus on gas dry reservoir characteristic & performance refer to the production and laboratory data. This work is also focused on evaluation for IGIP based on new data, drainage efficiency from current existing wells, assessment on surface facilities capabilities, success story of previous optimization jobs and next optimization plan.

I.4 Data and Methodology

In this study, the writer will use conventional petroleum engineering work for couple engineering work and 2 methods to evaluate IGIP with different approach as below:

a. Material Balance Method

In this method will use PVT data, geological & petrophysical data, pressure history to estimate IGIP & remaining gas reserve using MBAL software.

b. Decline Curve Method

In this method will calculate IGIP based on the decline history of production using OFM software.

Comparison the IGIP result from material balance method with decline curve method will determine the accuracy of IGIP calculation and it is also able to evaluate the efficiency of producer wells to drain the gas reserve in the “X” gas field.

I.5 Thesis Outline

The outline of the thesis will be divided in 5 chapters with additional attachments of data & calculation. Below are the outlines of the thesis:

1. CHAPTER I INTRODUCTION

This chapter will discuss the background of the study, purpose, scope of work, data & methodology and the outline.

2. CHAPTER II SUPPORTED THEORIES

This chapter will discuss supported theories related with natural gas characteristic, production and performance of gas reservoir and IGIP estimation method.

3. CHAPTER III GEOLOGY AND RESERVOIR CHARACTERIZATION

This chapter will inform about geological & stratigraphy and reservoir characterization of gas "X" field.

4. CHAPTER IV DATA CALCULATION AND ANALYSIS

This chapter will explain data accuracy, calculation and result, include the discussion of integrated study.

5. CHAPTER V CONCLUSION AND FUTURE WORK

This chapter will discuss the conclusion & recommendation refers to the integrated study results to be followed up for the next study and next jobs in the future.

CHAPTER II SUPPORTED THEORIES

II.1 Gas Reservoir

Gas reservoir is part of hydrocarbon reservoir where a mixture of different hydrocarbon molecules in varying composition. The type and amount of each molecular species in the gas determines the mixture properties at a given pressure and temperature.

Critical Temperature T_c is the temperature of a gas above which it can't be liquefied by increasing pressure.

Critical Pressure P_c is the pressure a gas exerts when in equilibrium with the liquid phase at the critical temperature.

Critical Volume V_c is the volume of one pound of gas at the critical temperature and pressure.

Cricondebar is the highest pressure at which a gas can exist.

Cricondenterm is the highest temperature at which a liquid can exist.

Bubble point is the pressure, at a given temperature, above which the mixture is 100% liquid.

Dew point is the pressure, at a given temperature, above which the mixture is 100% gas.

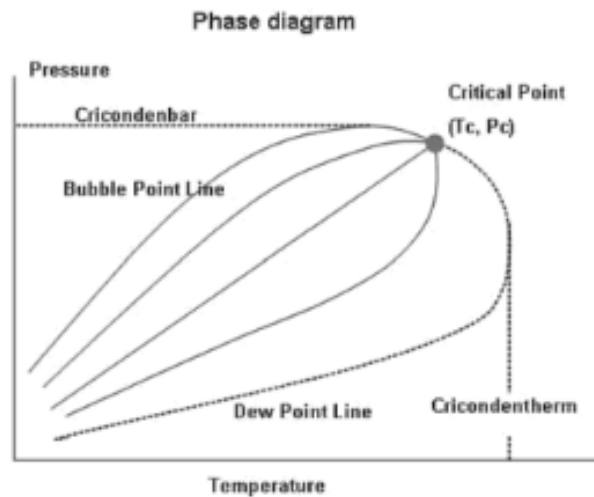


Figure 2-1 Typical gas reservoir phase diagram (James F. Lea 2008)

Dry gas reservoir is the hydrocarbon mixture exists as a gas both in reservoir condition and is also produced at surface condition. The definition of a dry gas reservoir is also showed by the amount of methane –pentane fraction.

II.2 Gas Fluid Properties

A gas is may defined as a homogeneous fluid that fill any container in which gas is placed. Generally, the natural gas is a mixture of hydrocarbon and non- hydrocarbon gases. To understand and predict the volumetric behavior of oil and gas reservoir as a function of pressure, knowledge of the physical properties of reservoir fluids must be determined. These fluid properties are usually measured at laboratory but in absence of experimentally measured properties, it can be derived from empirical correlations.

II.2.1 Gas Volume Formation Factor

The gas formation volume factor is used to relate the volume of gas, as measured at reservoir conditions, to the volume of the gas as measured at standard conditions, i.e., 60°F and 14.7 psia. This gas property is then defined as the actual volume occupied by a certain amount of gas at a specified pressure and temperature, divided by the volume occupied by the same amount of gas at standard conditions. In an equation form, the relationship is expressed as

$$Bg = \frac{V_{p,T}}{V_{sc}} \dots\dots\dots 2-1$$

- where Bg = gas formation volume factor, ft³/scf
- V_{p,T} = volume of gas at pressure p and temperature, T, ft³
- V_{sc} = volume of gas at standard conditions, scf

II.2.2 Gas Viscosity

The viscosity of a fluid is generally defined as the ratio of the shear force per unit area to the local velocity gradient. Viscosities are expressed in terms of poises, centipoise, or micro poises. One poise equals a viscosity of 1 dyne-sec/cm² and can be converted to other field Units.

The gas viscosity is not commonly measured in the laboratory because it can be estimated precisely from empirical correlations. Like all intensive properties, viscosity of a natural gas is completely described by the following function:

$$\mu_g = (p, T, y_i)$$

where μ_g = the viscosity of the gas phase.

The above relationship simply states that the viscosity is a function of pressure, temperature, and composition. Many of the widely used gas viscosity correlations may be viewed as modifications of that expression

II.2.3 Gas Compressibility Factor (z)

Gas compressibility factor, z , is a variable and its value depends upon the pressure, the temperature and the composition of the gas. This number is the magnitude of deviations of real gases from the conditions of the ideal gas law increases with increasing pressure and temperature and varies widely with the composition of the gas. Real gases behave differently than ideal gases.

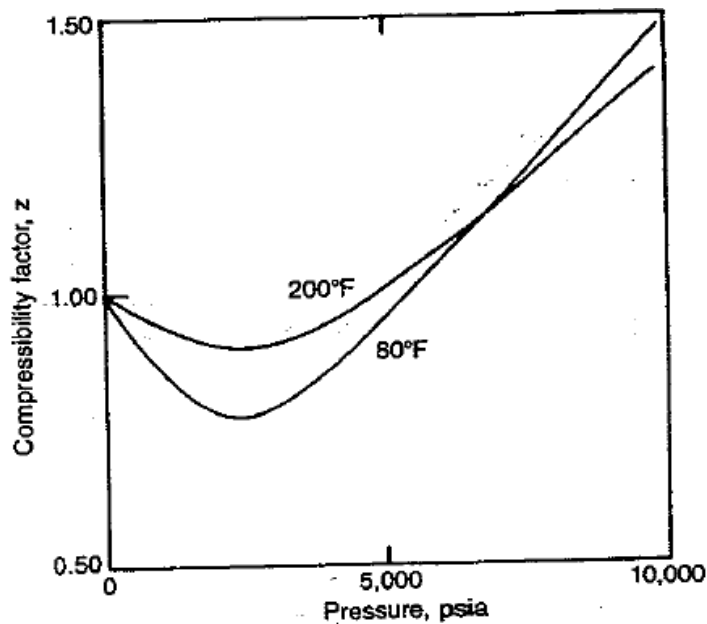


Figure 2-2 Compressibility factors for a natural gas as a function of pressure at constant temperature (Smith, 1990)

II.3 Well Deliverability

Well deliverability is defined as the ability of flow rate of the well against a specified pressure after a specified period of time following a specified shut-in-period.

Gas well testing is a series of tests, starting with the well shut in and with the shut-in pressure constant or nearly constant with time. Production pressures, temperatures, and rates of flow measured and recorded at specified time intervals after the well is opened to flow. Usually the time intervals are 0.5, 1, 2, 3, 6, 24, 48, 72 hours, etc. The result of gas well testing is good measures of well production performance over a period of years. It's also determined the properties of the reservoir such as rock physical properties and the completion characteristics of the well.

II.4 Initial Gas In Place Method

In this chapter, it explains couple methods to calculate *in place* for gas field. Method to calculate it among others are Material Balance and Decline Curves.

II.4.1 Material Balance Method

Material balance methods for estimating gas reserves are widely used and in general, are much preferred over volumetric methods where conditions are favorable and production information is available. The plot is consist of pressure divided by compressibility, p/z , against cumulative production on Cartesian coordinates. The simple material balance method illustrated by Figure 2-3 Pressure – production curve for a gas field on Cartesian coordinates below. During the evaluation using this curve, it must consider the effect of well in low-permeability reservoir, where pressure builds slowly after well is shut in. The effect of water influx on p/z cumulative gas production will also influence the curve type.

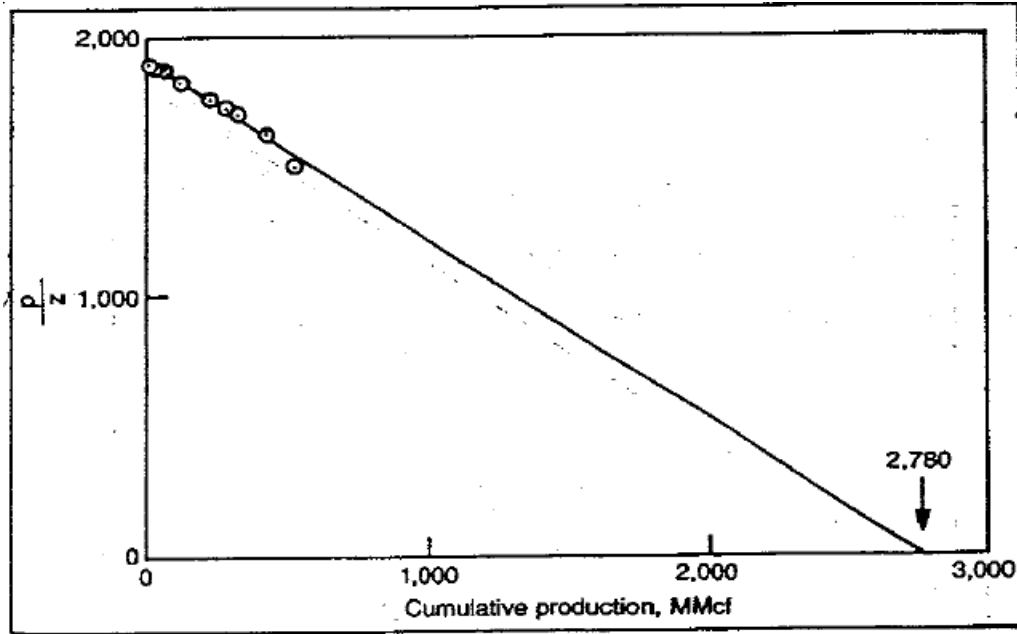


Figure 2-3 Pressure – production curve for a gas field on Cartesian coordinates (Smith, 1990)

II.4.2 Decline Curve Method

Production-decline analysis is the analysis of past trends of declining production performance, that is, rate versus time and rate versus cumulative production plots, for wells and reservoirs. Decline curves are one of the most extensively used forms of data analysis employed in evaluating gas reserves and predicting future production. The decline-curve analysis technique is based on the assumption that past production trends and their controlling factors will continue in the future and, therefore, can be extrapolated and described by a mathematical expression.

There are two type of decline curve analysis techniques, the classical curve fit of historical production data and the type curve matching technique.

Arps (1945) recognized the three types of rate decline behavior:

- **Exponential decline:** A straight line relationship will result when the flow rate versus time is plotted on a semi log scale and also when the flow rate versus cumulative production is plotted on a Cartesian scale.

- **Harmonic decline:** Rate versus cumulative production is a straight line on a semi-log scale; all other types of decline curves have some curvature. There are several shifting techniques that are designed to straighten out the curve those results from plotting flow rate versus time on a log-log scale.
- **Hyperbolic decline:** None of the above plotting scales, that is, Cartesian, semi-log, or log-log, will produce a straight-line relationship for a hyperbolic decline. However; if the flow rate is plotted versus time on log-log paper, the resulting curve can be straightened out with shifting techniques.

Nearly all conventional decline-curve analysis is based on empirical relationships of production rate versus time, given by Arps (1945) as follows.

$$q_t = \frac{q_i}{(1+b D_i t)^{1/b}} \dots\dots\dots 2-2$$

Where q_t = gas flow rate at time t , MMscf/day

q_i = initial gas flow rate, MMscf/day

t = time, days

D_i = initial decline rate, day⁻¹

b = Arps' decline curve exponent

(Exponential $b=0$, Hyperbolic $0 < b < 1$, Harmonic $b=1$)

The parameters determined from the classical fit of the historical data, namely the decline rate, D , and the exponent, b , can be used to predict future production. This type of decline-curve analysis can be applied to individual wells or the entire reservoir. The accuracy of the entire-reservoir application is sometimes even better than for individual wells due to smoothing of the rate data.

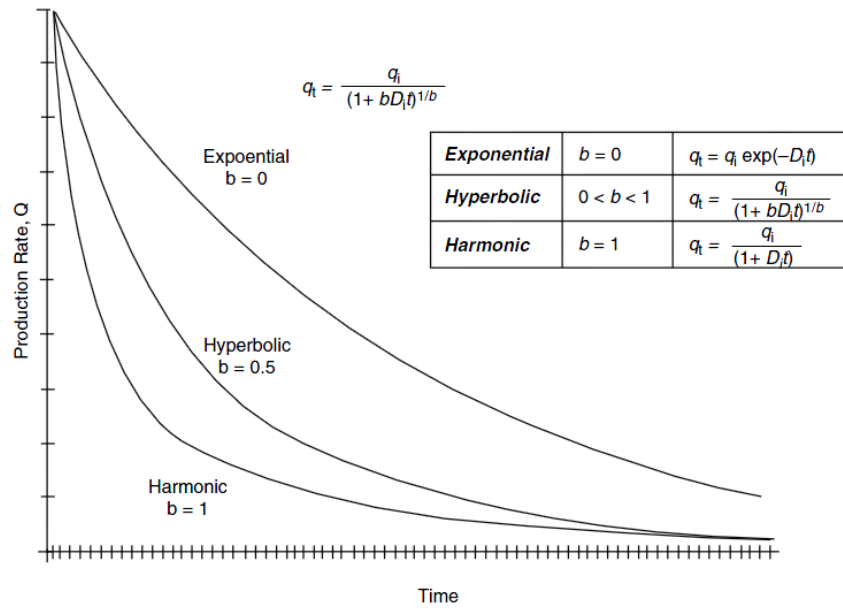


Figure 2-4 Decline curve rate / time (exponential, harmonic, hyperbolic) (Ahmed, 2006)

CHAPTER III GEOLOGICAL & RESERVOIR CHARACTERIZATION

III.1 Geology & Stratigraphy

III.1.1 Regional Geology

“X” gas field has produced gas and very little gas condensate since 2002. The “X” gas field is located in OK Block, in Palembang sub Basin, South of Sumatra, approximately 45 km south of Prabumulih, South Sumatra, covered \pm 25 km² of area. The gas field was discovered in December 1989 by drilling of Mdl-01 well, which tested 5 MMSCFD gas from Upper Baturaja Limestone. The area lies between the irregular unit boundaries which is bordered by PERTAMINA working area

JOB PERTAMINA-Talisman OK Ltd. was established in 1988 and has 4.630 km² working area. At first, JOB PERTAMINA-Talisman OK Ltd. was owned by PERTAMINA 50% and CNW (South Sumatra Ltd.) 50%. Talisman took the CNW (South Sumatra Ltd.) share in 1994. After 2nd relinquishment, the working area was changed to 1.155 km² at Kabupaten Muara Enim and 966 km² in Kabupaten Ogan Komering Ulu. See Figure 3-1 Location map of “X” gas field.

To the East, OK block is bordered by Lampung High, to the North is bordered by Tanjung Miring Timur High, to the West is bordered by Lematang Deep and to the South is bordered by a series of Paleozoic to Early Tertier rock outcropping.

This block has 3 structural lineaments those are:

- Northwest-Southeast trend that developed in Tanjung Miring Timur and Ogan as anticlinorium, at Kuang and Merbau area as fold structure associate with thrust fault.
- North – South trend that developed as deep in Eastern part of Beringin Field and Air Serdang as North – South fault pattern.

- Northeast – Southwest trend developed in the Cintamani Deep in the Eastern part and faulted block separated Kuang/Air Serdang High to Lematang Deep. Air Serdang-Guruh High is located between Cintamani deep and Lematang deep with the same structural orientation.

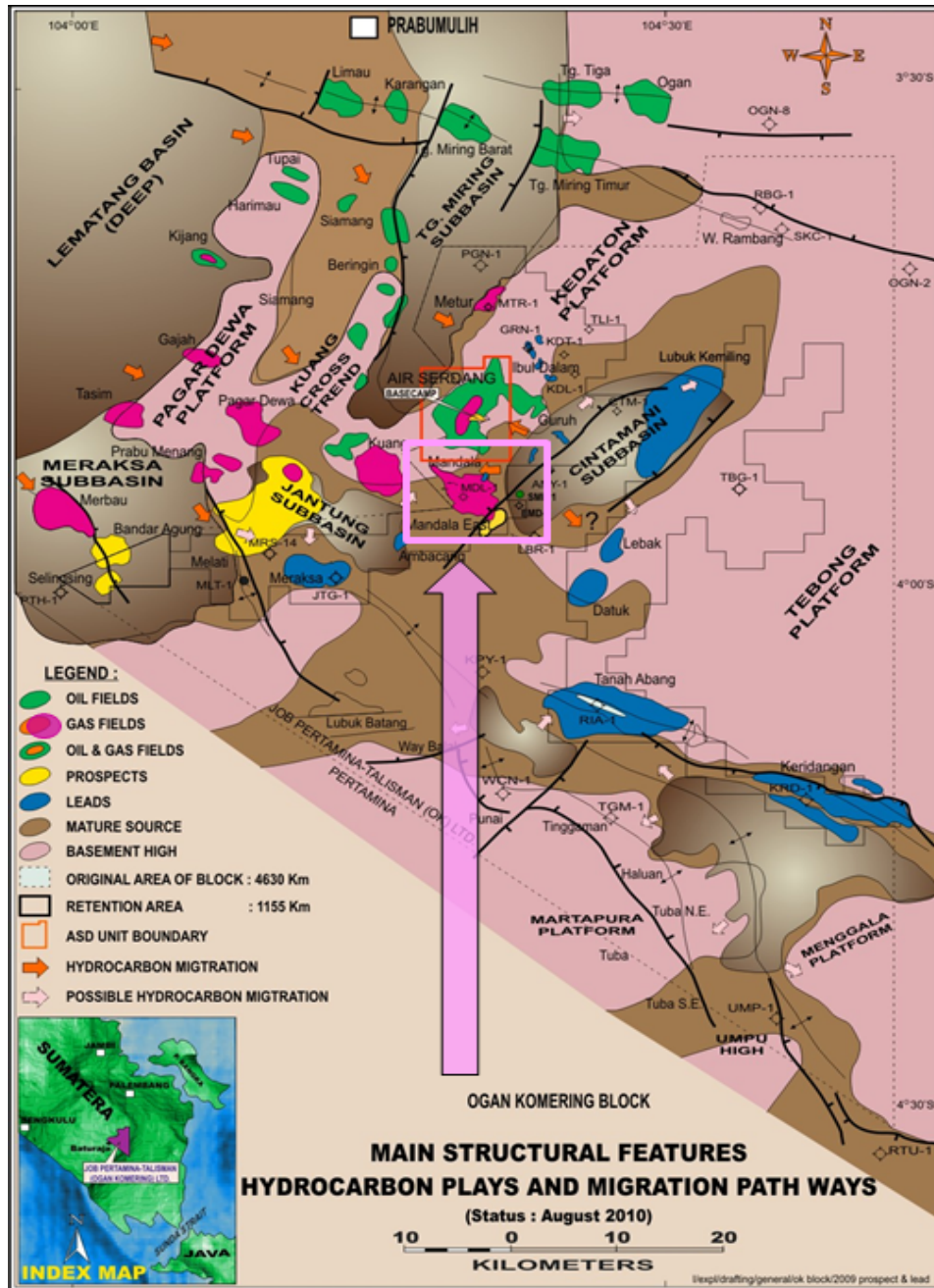


Figure 3-1 Location map of “X” gas field

Those structural patterns are similar with sea floor age in Indonesia Ocean, West of Sumatra Island to the South of Java Island. The sea floor age is a result of oceanic spreading in this area that is considered as responsible for plate movement from Gondwana land to the present day tectonic. According to Johnson et al (1976, in Soejono Martodjojo, 2002), the age of that sea floor are:

- Northwest-Southeast trend 130 – 80 mya or Paleozoic age.
- North – South trend 80 – 53 mya or Mesozoic age.
- Northeast – Southwest trend 53- 0 mya or Tertier and Quarter age.

The South Sumatra Basin is one of oil productive Tertiary back-arc sedimentary basins. The basement terraine of Sumatra is part of the ancient Sundaland Craton, which is composed as an amalgamation of microplates from different origin.

The tectonic that involved in Sumatra structural framework building can be separated in three events:

- The first event took place in Middle Mesozoic time when the collision between the Eurasian and the Indian plates reactivated weak zones and created the pull apart basin of South Sumatra.
- The second event took place in Late Mesozoic to Tertiary Miocene initiated extensive north-south crustal extension of horst and half graben in east of Beringin, Northeast – Southwest extension in Lematang and Cintamani graben and Northwest – Southeast extension in Merbau and Ogan – Tanjung Miring graben. These half-graben structures were then filled by sediments such as Lahat or Lemat and Talang Akar Formation (Eocene to Oligocene). In OK Block, some volcanic material of Lahat Formation accumulated as wedge-shaped graben filled adjoining northwest – southeast trending normal faults in Merbau deep and southern part of Cintamani deep. Post Lahat uplift was then occurred after Lahat deposition in the southern part of the block. The transgression took place in OK Block until Lower Miocene, creating Talangakar formation that deposited as channel sand deposit in deepest part of graben and following by sand wedging in high. The maximum transgression was marked by

development of Baturaja carbonate system in which reef grew in high area that facing to the open marine. The basin subsidence occurred until 2 Ma filled the clastic sediment of Gumai, Air Benakat and Muara Enim were deposited entire area.

- The third major orogenic which took place in Plio-Pleistocene time was the most important event in the OK Block area because it was dealing with present structure building.. Many old normal faults were rejuvenated as a thrust faults and made many of grabens (Merbau deep, Tanjung Miring – Ogan and Guruh North area) were inverted.

Different direction of strike of thrust in each block proved that this tectonic also related with block slip movement all along northeast – southwest regional fault in Cintamani and Lematang. Sediments associated with this tectonism consist of coarse clastic and volcanoclastic deposits (Kasai and Palembang Formations).

At the present situation, Merbau deep and Tanjung Miring Timur-Ogan deep appears as anticlinal high, while Air Serdang – Guruh old high became gentle sinclinal structure between those two high. Yet, since Air Serdang – Guruh is a very stable area. This structure became the best preservation for oil pool in this block.

III.1.2 Stratigraphy

The stratigraphy of “X” gas field contains seven lithostratigraphic units are described as follows refer to one of the well at “X” gas field.

Kasai Formation (0-332 m)

This formation is the youngest Tertiary sediment encountered in MDL-3 well, and was dominated by sandstone with streaks of claystone and siltstone. **The sandstones** are clear, translucence, offwhite, friable, loose, locally consolidated, coarse to very coarse grains, locally conglomeratic, angular to subangular, medium to poorly sorted, non-calcareous, poor intergrains to no visible porosity, trace of pyrite, chert, abundant of glauconite, locally with volcanic materials, and mafic minerals, no oil shows. **The claystones** are green,

greenish grey, soft, soluble in a part, occasionally firm to moderate hard, locally earthy, locally silty, subblocky, non-calcareous, and trace of pyrite. **The siltstone** are greenish grey, green, light grey, soft, locally firm to moderate hard, subblocky, subfissile, sandy, non-calcareous, trace of carbon streaks.

Muara Enim Formation (332 – 816 m)

This formation consisted of interbedded sandstone, claystone and siltstone in the upper part and interbedded sandstone, claystone, siltstone, coal and shale in the lower part. **The sandstones** are clear, off-white, translucence, friable, loose, medium to coarse grains downward, locally conglomeratic, subangular to angular, well to medium sorted, non-calcareous cemented, no visible porosity, clear crystalline quartz, volcanic materials, abundant of glauconite, trace of carbon specks, no oil shows. **The claystones** are greenish grey, grey, green, light grey, soft, soluble, sticky in a part, subblocky, subfissile, non-calcareous, trace of carbon streaks, abundant of glauconite. **The coals** are black, dark brown, soft, brittle, fissile, firm, occasionally blocky, conchoidal fracture, vitreous lustre, woody structure, trace of pyrite, and commonly lignite. **The shales** are light brown, dark grey, light grey, soft, firm, moderate hard in a part, platy, subfissile, occasionally sticky, silty, non-calcareous, trace of carbon streaks, occasionally interlaminated with dark minerals.

Air Benakat Formation (816 – 1171 m)

Air Benakat Formation consists of interbedded shale and siltstone with streaky of sandstone, dolomite, limestone and thin streaky coal in the upper part. **The shales** are greenish grey, green, dark grey, light grey, soft to firm, locally brittle, subfissile to fissile, subplaty to platy, locally silty, non-calcareous, abundant of fine pyrite, trace of carbonaceous streaks, locally trace of forams and locally trace of calcite. **The siltstones** are greenish grey, brownish grey, dark grey, light grey, green in part, soft to firm, platy, subfissile, locally subblocky, sandy to slightly sandy, grading to very fine sandstone in part, slightly calcareous, trace of pyrite, carbonaceous streak, locally trace of calcite vein and locally trace of forams. **The sandstones** are colorless, light grey, off-white, occasionally

translucence, friable, consolidated, locally loose, very fine to fine grain, medium grain downward, subrounded to subangular, moderately to well sorted, slightly calcareous cemented, fair to good intermatrix visible porosity, quartz, glauconite, mafic minerals in part, trace of carbonaceous streaks and no oil shows. **The coals** are black, dark brown, firm, brittle, subfissile, occasionally blocky, conchoidal fracture, woody structure, vitreous lustre and trace of pyrite. **The dolomites** are brownish grey, olive grey, light brown, brownish yellow, locally buff, medium hard to hard, locally brittle, microcrystalline to recrystalline, aphanitic, mudstone, commonly tight, growth, glauconite infill, trace of coral and no oil shows. **The limestones** are brownish yellow, brown, olive grey, cream in part, medium hard to hard, brittle in part, microcrystalline to recrystalline, mudstone, aphanitic, commonly tight, no visible porosity to trace of micro vuggy porosity, glauconite infill, trace of coral, no fluorescence and no oil shows.

Gumai Formation (1171 - 1493 m)

The Gumai Formation is dominantly consists of interbedded shale and siltstone with streaky sandstone, dolomite and limestone. **The shales** are greenish grey, dark grey, light grey, soft to firm, occasionally brittle to moderate hard, subfissile to fissile, platy, locally silty, sticky in part, calcareous, dominantly shale marly in the upper part, trace of carbonaceous streaks, trace of forams, abundant of fine pyrite, trace of calcite vein and commonly marly. **The siltstones** are greenish grey, grey, brownish grey in part, soft, firm, fissile to subfissile, subblocky, micro mineral lamination, sandy, grading to very fine sandstone, calcareous with trace of halite, glauconite, trace of forams, carbonaceous streaks, trace of calcite vein, abundant of fine pyrite, commonly associated with marly. **The sandstones** are commonly light grey, colourless, off-white, translucence in part, friable, consolidated, loose in part, fine to very fine grain, subrounded to subangular, moderate sorted, calcareous cemented, fair intermatrix visible porosity, quartz, glauconite, trace of mafic minerals, trace of carbonaceous specks, no fluorescence and no oil shows. **The dolomites** are buff, olive grey, brownish yellow, moderate hard to brittle, microcrystalline, recrystalline, aphanitic, mudstone, occasionally dolomitic limestone, no visible porosity,

commonly tight, glauconite infill, no visible porosity, sandy, trace of corals, trace of pyrite, trace of quartz rework and no oil shows. **The limestones** are olive grey, buffalio, cream in part, brownish grey, locally off-white, moderate hard to hard, brittle in part, dense, slight opaque, microcrystalline, recrystalline in part, mudstone to dolomitic, commonly tight, no visible to trace of micro vugular porosity, glauconite infill, trace of corals, trace of quartz rework, no fluorescence, no stain and no oil shows.

Baturaja Formation (1493 – 1566 m)

This formation consists of limestone with streaky of shale. **The limestones** are brownish yellow, buffalio, olive grey, cream, off-white, hard to moderate hard, brittle, chalky in part, microcrystalline to recrystalline, crystalline to sucrosic texture, wackestone, packstone, boundstone, micro vuggy to intercrystalline visible porosity, trace of crystalline quartz, trace of argillaceous, calcite growth, dull to dark brown fluorescence, very slow to trace of orange pale yellow streaming cut, no odor, no stain, trace of light yellow residual and gas shows. **The shales** are dark grey, brownish grey, light brown, occasionally light grey, soft to firm, occasionally moderate hard to hard, fissible to subfissile, platy, streaky in part, calcareous, disseminated fine pyrite, trace of forams, trace of calcite vein, trace of carbonaceous streaks and commonly marly.

Talang Akar Formation (1566 –1639 m)

The Talang Akar formation is dominated by shale interbedded with siltstone, sandstone, limestone and streaky of coal called as **Talang Akar Shale** (1566 –1586m), and occurrences of domination sandstone layer and interbedded between siltstone and shale with streaky coals called as **Talang Akar Sand** (1586-1639 m). **Talang Akar Shale:** **The shales** are dark grey, greenish grey, dark green, occasionally light brown, moderate hard to firm, brittle, fissile to subfissile, platy, blocky, silty downward, calcareous, abundant of fine pyrite, trace of forams with carbonaceous streaks. **The sandstones** are light grey, greenish grey, colorless to off-white, dirty, consolidated, friable in part, fine to medium grain, subrounded to subangular, medium to poor sorted, calcareous

cemented, poor intergrain to intermatrix visible porosity, trace of carbonaceous streaks, abundant of fine pyrite, mafic minerals, no fluorescence and no oil and gas shows. **The limestones** are brownish grey, olive grey, pale yellow, occasionally buffaloe to off-white, hard to very hard, recrystalline, cryptocrystalline, grainstone, commonly tight, trace of intercrystalline visible porosity, disseminated pyrite, trace of coral, no fluorescence and no oil shows. **Talang Akar Sand:** **The sandstones** are dark grey, brownish grey, colorless to off white, light grey, occasionally translucence, consolidated, friable, brittle, moderate hard, medium to fine grains, sub-rounded to subangular, well to medium sorted, non-calcareous cemented, poor to fair intergrains visible porosity, locally thin streaky shally, trace of pyrite, trace of mafic minerals, dull to dark brown to pale yellow fluorescence, milky white to pale yellow, slow to very slow streaming crushed cut, no to trace of brown oil stain, trace of to poor oil shows. **The shales** are dark grey, brownish grey, light brown, occasionally light to brown, firm, locally moderate hard to hard, fissile to subfissile, platy, sticky in part, calcareous, disseminated with fine pyrite, trace of forams, trace of carbonaceous streaks and commonly marly. **The siltstones** are brownish grey, dark grey, dark green, moderate hard to hard, firm, platy, subfissile to fissile, sandy, grading to very fine grain sandstone, slightly calcareous to non-calcareous, abundant of fine pyrite and carbonaceous streaks.

Lahat Formation (1639 – 1662 m)

This formation consists of sandstones and conglomerates. The sandstones are colorless, off-white, translucence to colorless, friable, brittle, consolidated moderate hard to hard, medium grain to coarse grain, conglomeratic downward, with quartzite fragments, subangular to angular, locally subrounded, poor sorted, non-calcareous cemented, quartz, pyrite infill, crystal to lithic tuff, mafic minerals, volcanic materials, poor to trace of intergranular visible porosity, no stain, no odor and no oil shows. **The Conglomerates** are off-white to colorless, light grey, very hard to hard, coarse to cobble, sandstone as grainmass, subrounded to rounded, variable streated, non-calcareous, quartz fragment, mafic

minerals, lithic tuff, occasionally volcanic materials, lithic tuff, occasionally carbonaceous streaks, commonly tight, no visible porosity and no oil shows.

Basement (1662- 1682 m/TD)

This zone consists of metaquartz and slate. **The metaquartz** are white to off white, translucent in part, occasionally colorless, cloudy, compact to hard, very hard, coarse to medium grain, granoblastic, intergrowth, quartzite, pyrite, commonly tight to no visible porosity and no oil shows. **The slates** are light grey, dark grey, locally greenish grey, moderate hard to hard, fissile, slaty cleavage, lepidoblastic, silky to silver luster, tight, no visible porosity, intercalation with metaquartzite in part.

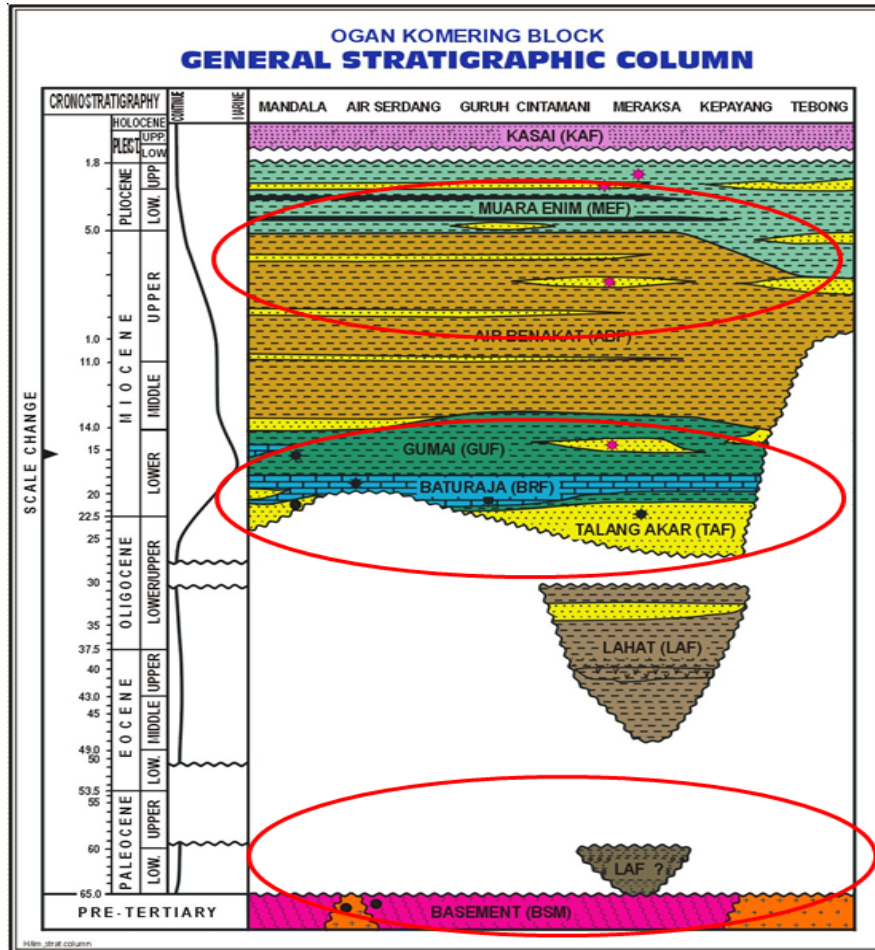


Figure 3-2 General stratigraphic of “X” gas field

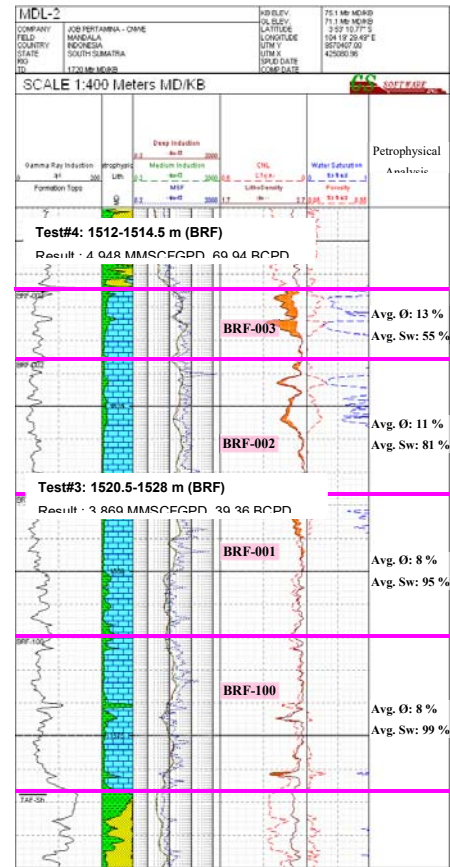
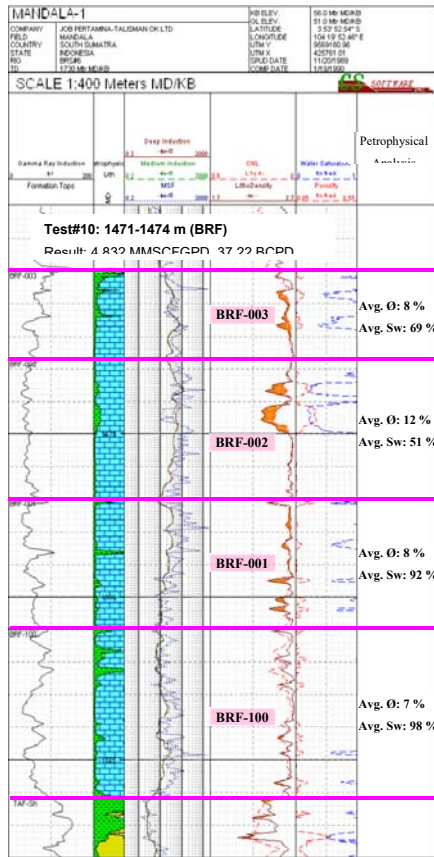


Figure 3-3 Typical log of “X” gas wells

III.2 Reservoir Characterization

III.2.1 Reservoir Fluid Properties Analysis

The fluid properties used in the study is obtained from results of PVT study of samples from the MDL-1, MDL-2 and MDL-3 wells. Results of the PVT study are summarized in Attachment 1, Attachment 2 and Attachment 3. Figures 3-4 shows pressure variations of Z. These fluid properties are used as input data for the field material balance calculation.

Fluid composition and properties from laboratory experiments may be used to identify the reservoir fluid. It is shown in Attachment 1, the methane plus ethane concentration is 84.72 % mole, the heptanes plus concentration is 0.95 % mole, and the total impurities of CO₂, H₂S, and N₂ concentration is 11.26 %

mole which is considered rather high. Thus, the reservoir fluid indicates a dry gas. The initial gas formation volume factor and the specific gas gravity are 0.008 cu ft / SCF and 0.7597, respectively.

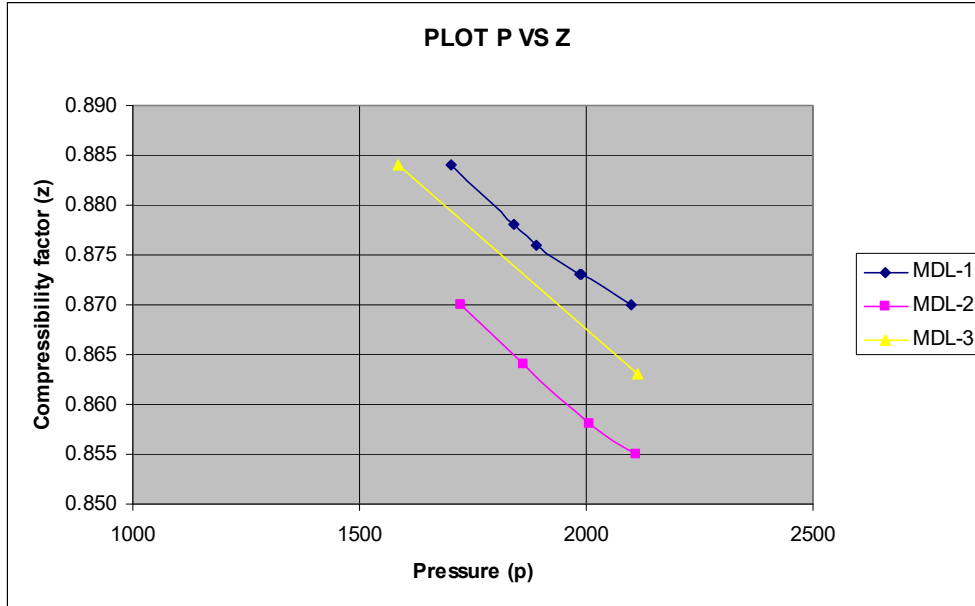


Figure 3-4 Plot of pressure vs compressibility factor

III.2.2 Core Rutin Analysis

The samples used in the analysis are sidewall and conventional cores extracted from MDL-2 well. The samples were taken from an interval depth of 1510.68 – 1519.56 m-MD. The horizontal permeability and porosity data at corresponding depths are used to construct permeability vs. porosity cross-plots. The permeability-porosity correlation used as reservoir data was derived from Figure 3-5 Plot of permeability versus porosity, from which it was found that that permeability could be correlated with porosity using the following equation:

$$K=(0.0009) e^{0.6308\phi} \dots\dots\dots 3-1$$

In addition to permeability and porosity, routine core analysis also includes water saturation determination.

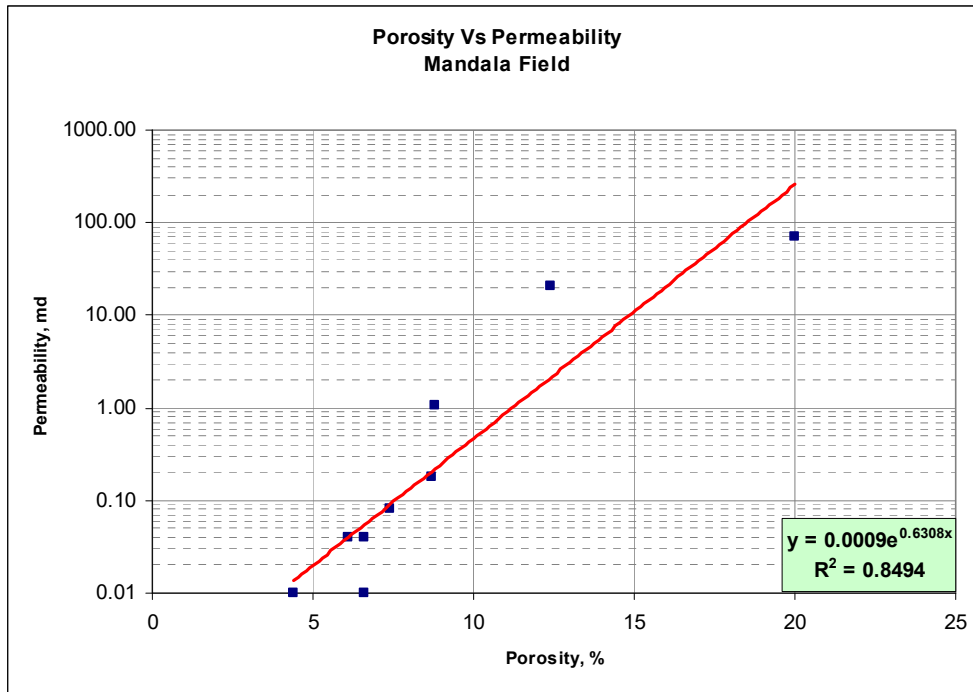


Figure 3-5 Plot of permeability versus porosity

III.2.3 Log Interpretation

A Summary of the log interpretation results is shown in Attachment 6 Summary of log interpretation result. The values of porosity from log interpretation are within the range of 5.4 – 13.43 %. Furthermore, the constraint value of 20 % is used as a maximum porosity in reservoir model which is considered a maximum porosity value obtained from the core analysis.

CHAPTER IV DATA CALCULATION AND ANALYSIS

In this chapter, it calculates and analyses the production and reservoir data of “X” gas field. By using the calculation results, it can calculate Initial Gas In Place (IGIP), drainage area each wells, production optimization through lower down the compressor staging till very low reservoir abandonment.

IV.1 Data Calculation

IV.1.1 Reservoir Pressure And Temperature

Determination of initial reservoir pressure is very important because in PVT analysis will refer to initial reservoir pressure and its change during the field life. The initial reservoir condition is mentioned as initial reservoir pressure (P_i) and initial reservoir temperature (T_i). During the production process, reservoir pressure will decrease meanwhile reservoir temperature is assumed constant (isotherm condition). Both initial reservoir pressure and temperature can be obtained by running the pressure & temperature gauge during exploration well.

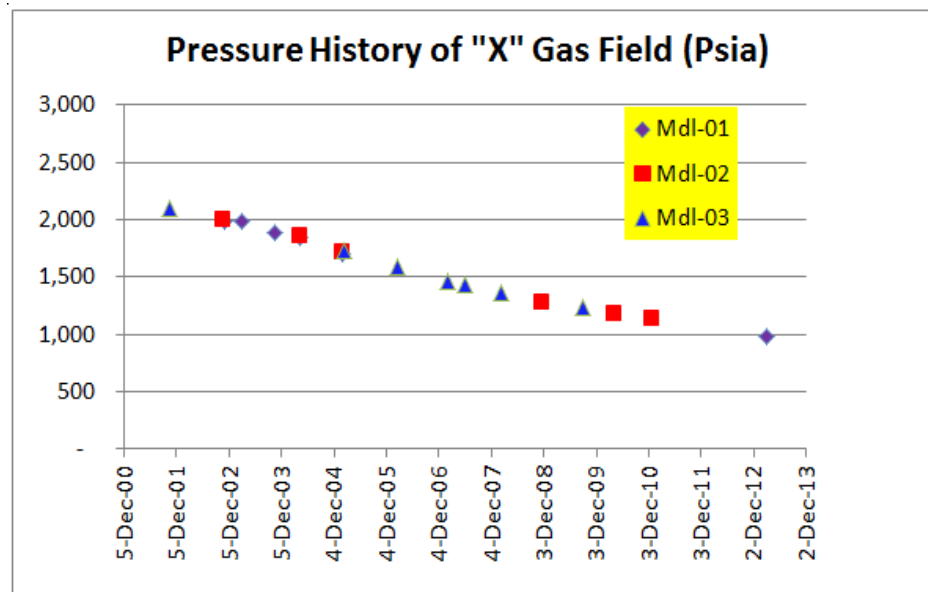


Figure 4-1 Reservoir pressure of “X” gas field vs. time

Depleting reservoir pressure can also be monitored by plotting the relationship between pressure vs time where the history reservoir pressure is obtained by routinely reservoir pressure monitoring program.

Refer to the plot of figure 4-1 Reservoir pressure of “X” gas field, initial reservoir pressure is 2111 psia. During the production period, reservoir pressure of “X” gas field depleted till 981 psia in February 2013 as shown in attachment 7 “X” gas field pressure history record.

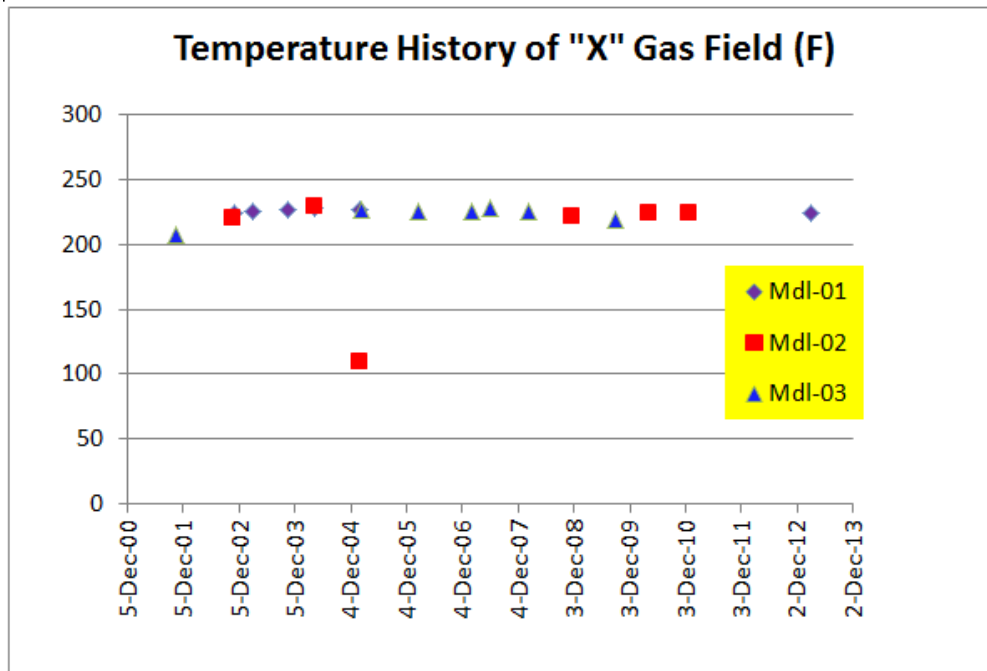


Figure 4-2 Reservoir temperature of “X” gas field versus time

From figure 4-2, it can be predicted or measured that initial reservoir temperature is 228 F. There is not much changing of reservoir temperature during the production depletion and it is considered as isotherm process in reservoir.

IV.1.2 Reservoir *Cut-Off*

Refer to core routine analysis data and log interpretation, the porosity range is 5.4 – 13.43 % and permeability (K) is 1 m Darcy. Detail routine core

analysis is shown in attachment 5 or figure 3-5 meanwhile for log interpretation is in attachment 6.

IV.1.3 Production Performance & Well Deliverability

Production performance plot between rate, cumulative production and pressure versus time of “X” gas field can be shown at figure 4-3 below.

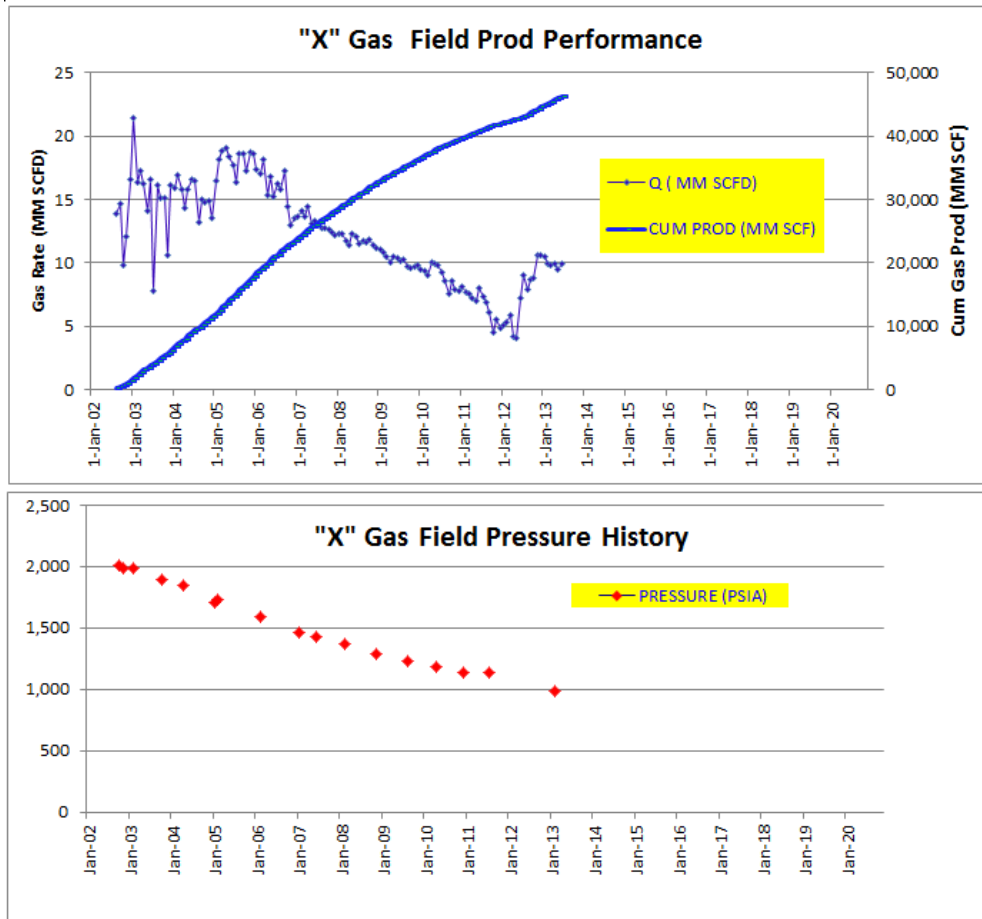


Figure 4-3 Production and reservoir pressure history of “X” gas field

“X” gas field has produced since 2002 from 3 active producer wells, namely Mdl-01, Mdl-02 and Mdl-03. During the first production, those 3 wells were choked until year 2006 when chokes were opened. Since then, those 3 wells produced natural flows and have been declined naturally. In January 2010, 2

compressors were installed with suction pressure 550 psig and discharge pressure 964.7 psig. Those compressors are designed for 110 % of the remainder of the gas over and above 20.0 MMSCFD necessary to achieve the total throughput, or 15.0 MMSCFD, whichever is greater. After Mandala compressor installation, only a little bit increase of gas production, because the well head pressure of the wells have been reached between 680 psig – 720 psig and pressure at downstream of slug catcher was about 635 psig.

In mid of 2012, lowering suction pressure of those compressors to 200 psig suction pressure have increased the production from about 5 MM SCF to 10 MM SCF. The increasing of gas production is contributed from all 3 wells; Mdl-01, Mdl-02 and Mdl-03. Currently, WHP in “X” gas field is between 411 psig – 462 psig, manifold (satellite) pressure is 400 psig and downstream of slug catcher is about 380 psig.

IV.2 Analysis

Based on the reservoir and production data as explained and calculated previously, the calculation of IGIP, drainage efficiency and field production optimization can be calculated and evaluated.

IV.2.1 Reservoir Type

The PVT from laboratory study results of Mdl-01 as attached on attachment 1 and other PVT laboratory test, combined with production data of “X” gas field to determine the type of gas reservoir. Refer to William D. McCain on JPT in September 1994 “Heavy Components Control Reservoir Fluid Behaviour”, “X” gas field is categorized as a dry gas reservoir. See figure 4-4 PVT laboratory result and production data that determines “X” gas field as a dry gas reservoir. The effect of condensate volume on reservoir gas specific gravity and on cumulative gas production are insignificant when the yield of condensate is 10 bbl/MMSCF or less (i.e., when the initial producing GOR is 100,000 SCF/STB or more). Even though some condensate is produced to the surface and possibly some retrograde condensate is formed in the reservoir, reservoir fluid with initial producing GOR’s this high can be treated as dry gases, while the GOR of

“X” gas field is higher than 100,000 SCF/STB and mol % heptanes plus is less than 0.7%. By this fact, the treatment of dry gas reservoir is applied to “X” gas field. The analysis and formula that governs the correlation and calculation of “X” gas field to estimate IGIP etc. will consider for dry gas reservoir condition.

Reservoir Type Of “X” Gas Field~ “DRY GAS RESERVOIR”

Attachment 1 PVT study of samples from the MDL-1

Component	Separator		Well Stream	
	Liquid Mol%	Mol%	Mol%	GPM
Hydrogen Sulfide	0	0	0	
Carbon Dioxide	3.71	8.39	8.35	
Nitrogen	0.26	2.87	2.85	
Methane	19.11	81.68	81.11	
Ethane	2.66	3.04	0.812	3.04
Propane	4.98	2.1	0.577	2.13
Iso-Butane	1.49	0.31	0.102	0.32
N-Butane	3.16	0.5	0.157	0.52
Iso-Pentane	2.52	0.23	0.085	0.23
N-Pentane	2.49	0.19	0.068	0.21
Hexanes	6.1	0.22	0.09	0.27
Heptanes	13.65	0.26	0.096	0.38
Octanes	17.37	0.15	0.068	0.31
Nonanes	9.71	0.04	0.019	0.13
Decanes	5.88	0.01	0.008	0.06
Undecanes	3.07	0.01	0.004	0.04
Dodecane	1.54	0	0.002	0.013
Tridecane	0.9	0	0.001	0.007
Tetradecane	0.53	0	0	0
Pentadecane	0.43	0	0	0
Hexadecane	0.12	0	0	0
Heptadecane	0.05	0	0	0
Octadecane	0.04	0	0	0
Nonadecane	0.01	0	0	0
Eicosane plus	0.02	0	0	0
Total	100	100	2.086	100

Properties of Heptane Plus :			
*API Gravity at 60°F	49.5		
Density, gm/cc	0.7818	0.737	0.7597
Molecular Weight	111.8	103	107.4

Refer to : William D. McCain, 1994

	Black Oil	Volatile Oil	Retrograde Gas	Wet Gas	Dry Gas
Initial producing gas/liquid ratio, scf/STB	<1,750	1,750 to 3,200	>3,200	>15,000*	100,000*
Initial stock-tank liquid gravity, °API	<45	>40	>40	Up to 70	No liquid
Color of stock-tank liquid	Dark	Colored	Lightly colored	Water white	No liquid

*For engineering purposes.

	Black Oil	Volatile Oil	Retrograde Gas	Wet Gas	Dry Gas
Phase change in reservoir	Bubblepoint	Bubblepoint	Dewpoint	No phase change	No phase change
Heptanes plus, mol%	>20%	20 to 12.5	<12.5	<4*	<0.7*
Oil FVF at bubblepoint	<2.0	>2.0	—	—	—

*For engineering purposes.

- ✓ TOTAL C7+ = 0.47 (Ref Table-2)
- ✓ GOR >= 100,000 (Ref Table-1 : Field Production data)

Figure 4-4 PVT laboratory result and production data that determines “X” gas field as dry gas reservoir

IV.2.2 Material Balance Method

Using the commercial petroleum software, the estimation of initial gas in place is related with aquifer volume. There are 2 methods are straight line and regression applied. The straight line method can be applied if there is no presence of water influx, but the regression is more accurate if there is presence of water influx.

By using this software, there are couple steps to fill the data, such as figure 4-5 below. By using the PVT data of “X” gas field, gas deviation factor can be calculated using correlation as figure 4-6.

The screenshot shows a software window titled "Gas - Black Oil: Data Input". It features a toolbar with icons for Done, Cancel, Help, Match, Table, Import, Export, Calc, and Match Param. The main area is divided into two sections: "Input Parameters" and "Correlations".

Input Parameters:

Gas gravity	0,7597	sp. gravity
Separator pressure	114,696	psia
Condensate to gas ratio	0	STB/MMscf
Condensate gravity	49,5	API
Water salinity	10000	ppm
Mole percent H2S	0	percent
Mole percent CO2	3,71	percent
Mole percent N2	0,26	percent

Correlations:

Gas viscosity: Lee et al (dropdown menu)

Use Tables
 Use Matching
 Model Water Vapour

Figure 4-5 Fluid properties data to generate MBAL model

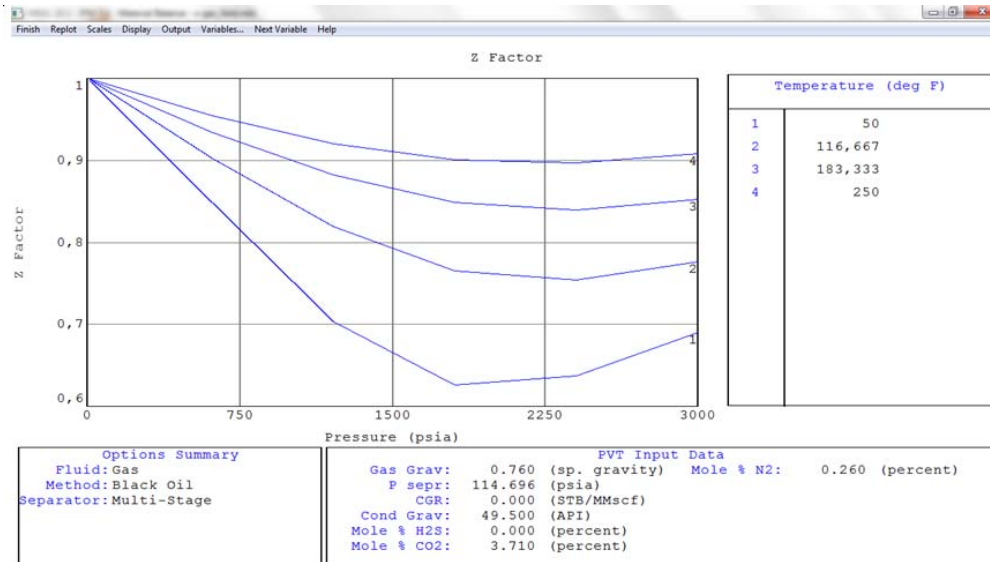


Figure 4-6 Gas deviation factor (Z) of “X” gas reservoir refer to MBAL model

Refer to the geological condition and reservoir characteristic, “X” gas field is considered as one reservoir (tank) because mostly is produced from BRF-003 at those 3 active producer wells. There is no compartmentalization. By Inputs production data & reservoir pressure history, pressure history matching process can be done. As a result shown by figure 4-7, those 3 parameters of actual reservoir pressure, simulation and predictions are matched. The depletion of reservoir pressure is purely due to the expansion of fluid and rock properties, therefore no presence of water influx is detected. By having the matching history, running the model can be processed and show the result as figure 4-8 that estimates initial gas in place of “X” gas field.

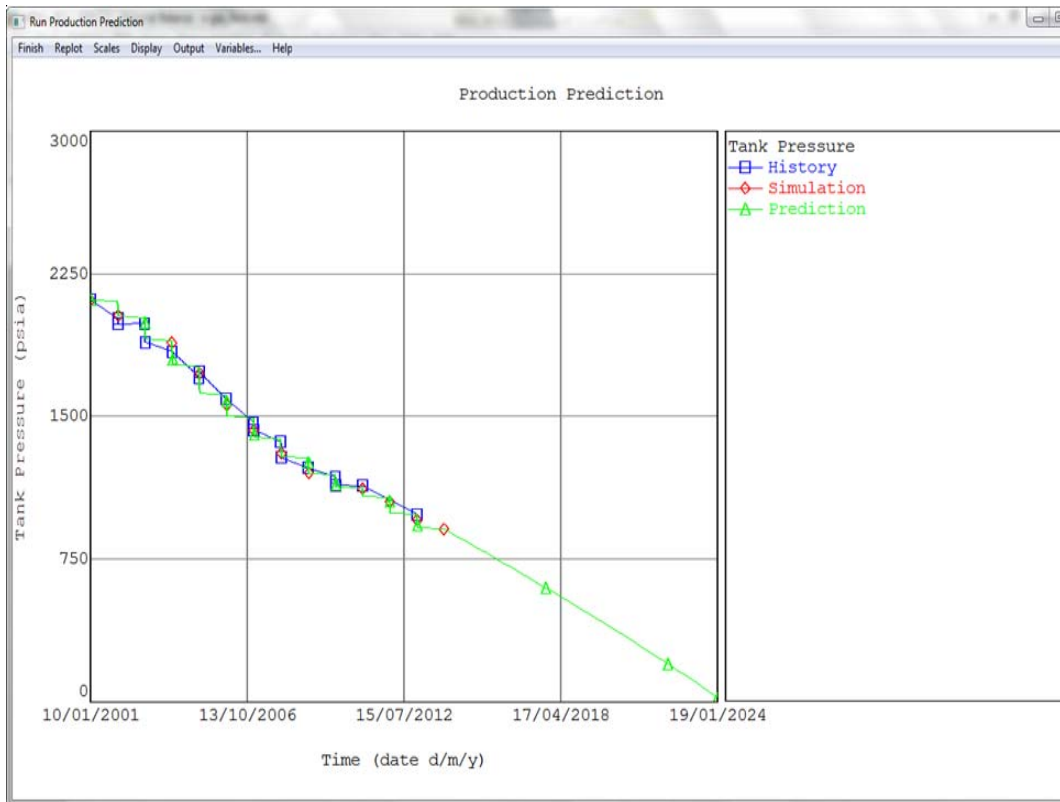


Figure 4-7 History match of reservoir pressure, simulation and prediction

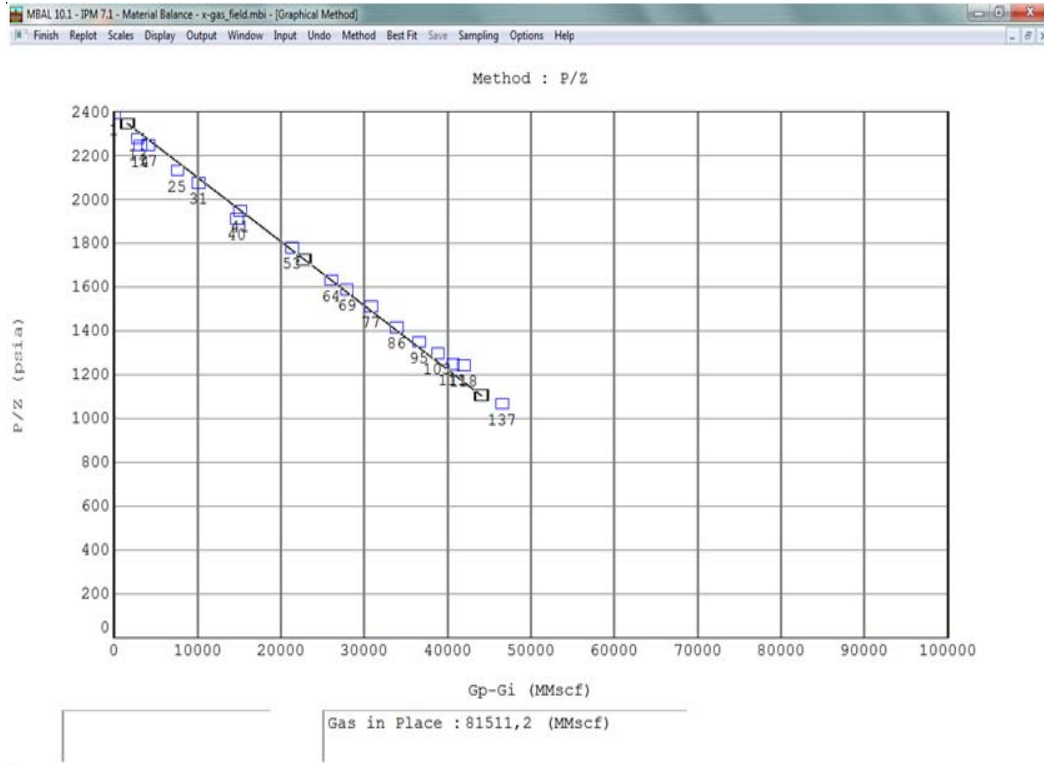


Figure 4-8 Straightline MBE method for IGIP “X” gas field

Meanwhile figure 4-9 determines “X” gas field drive mechanism that gives the dominant impact in its drainage process.

The same method is also applied to each wells for Mdl-01, Mdl-02 and Mdl-03. The results give the good value of IGIP where the matching process of reservoir pressure history show the closed result between the actual data with simulation and prediction data. The attachment of MBE results using MBAL for each wells are attached in attachment 14, 15 & 16.

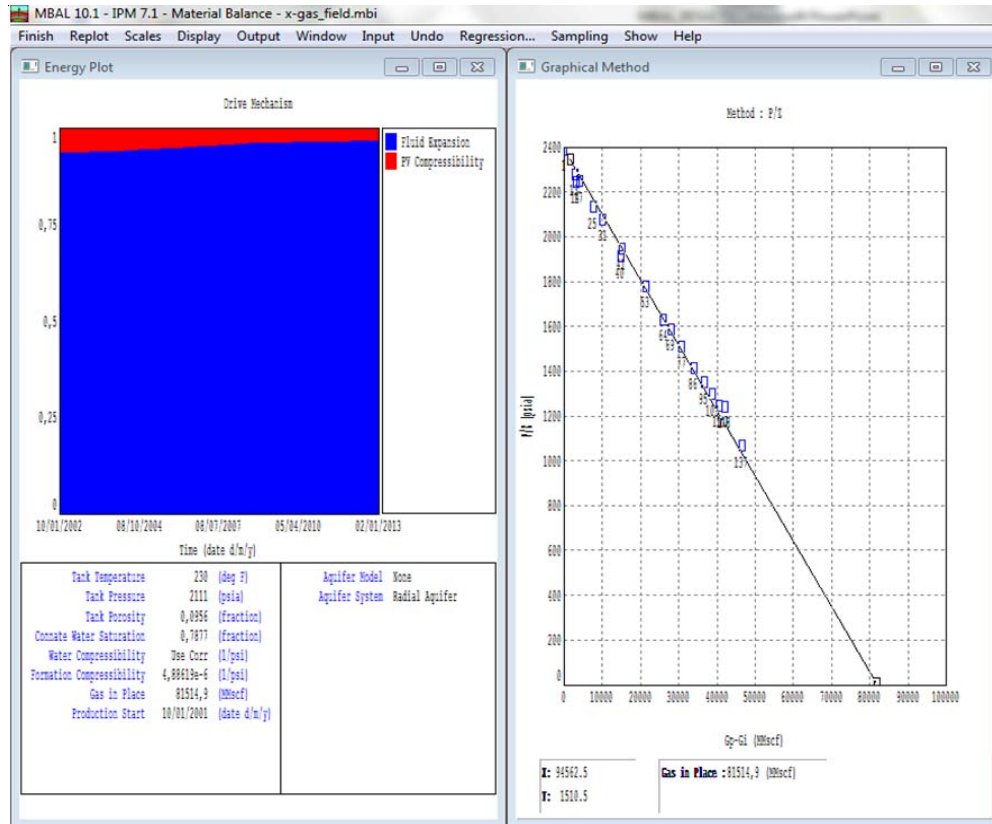


Figure 4-9 Dominant drive of “X” gas field

IV.2.3 Decline Curve Method

This method also utilizes the commercial petroleum software, namely OFM. By giving the production data history and plotted versus time in semi-log, conventional decline curve of exponential type is very match with the requirement. This method has the weaknesses in sensitivity of production history influenced by history of workover or wellservice activities in wells or other activities that influence the production history. If there will be potential activities to increase the production which is not executed yet, decline curve method will show the lower result of Estimated Ultimate Recovery (EUR) value, it means the IGIP value will be smaller than actual value. Total of IGIP calculation using this method is also influenced by limited of economic final rate, so the IGIP’s value is more reflected by EUR value which will give smaller value as shown in figure 4-10.

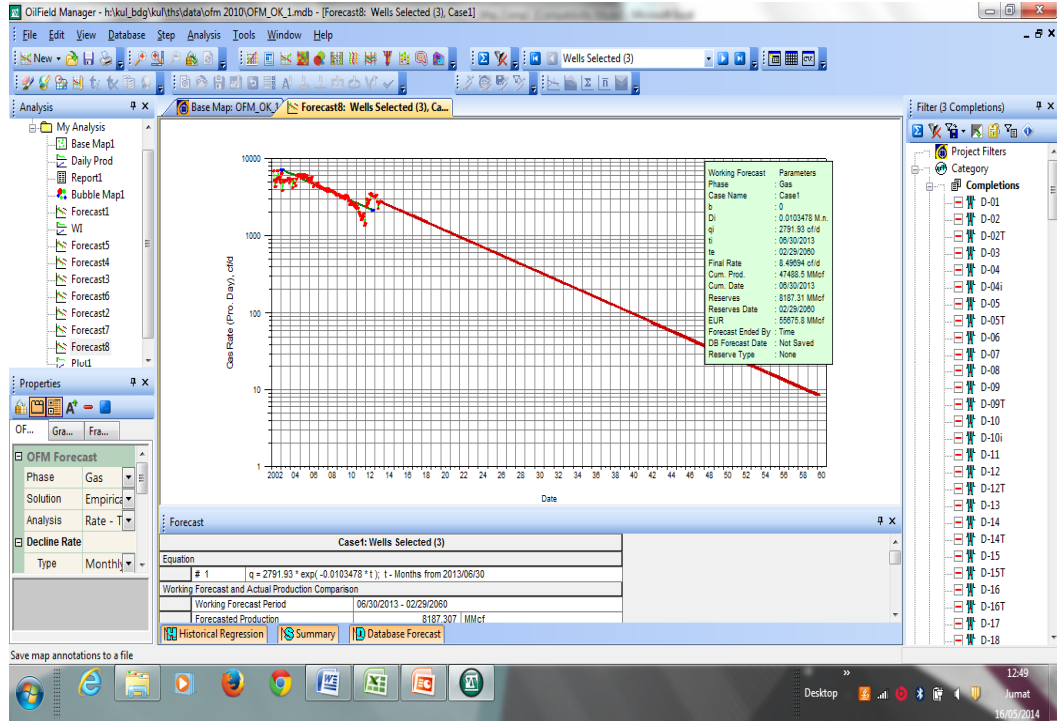


Figure 4-10 Decline curve method of “X” gas field

The complete IGIP result of each wells using decline curve method are attached in attachment 17, 18 & 19.

IV.2.4 Results Based On Methods

After getting the IGIP value, the next step is to compare IGIP value estimated by different methods. Additional information of IGIP estimated by Static model & Dynamic model which refer from previous internal study are also compared.

- IGIP MBal of field : 81,5 BSCF
- IGIP MBal of well by well : 82.3 BSCF
- IGIP Decline Curve of field : 55.7 BSCF
- IGIP Decline Curve of well by well : 67.4 BSCF
- IGIP of Static Model : 81.4 BSCF
- IGIP of Dynamic Model : 81.1 BSCF

Table 4-1 IGIP MBal analysis by well and IGIP Decline Curve by well

Well	Mbal (BSCF)	Decline Curve (BSCF)
Mdl-01	25.2	24.4
Mdl-02	26.3	21.8
Mdl-03	30.8	21.2
Total	82.3	67.4

From the estimation result, IGIP material balance is very close with IGIP from static simulation & dynamic simulation from previous in house study by the company, meanwhile IGIP from decline curve method is lower than those 3 methods. This smaller IGIP value from decline curve analysis is caused by couple conditions, among others:

- The current production data used for the estimation is limited by the actual production up to now where suction pressure of compressor is still 200 psia. It will give the smaller production rate, smaller reserve covered and smaller IGIP estimation due to not optimal production yet.
- The IGIP value is represented by estimated ultimate recovery, since in decline curve method, it is limited by the minimum final rate that can't decline the well / field until 0 rate.
- No optimization yet such as WO/WS activities and lowering the lowest compressor pressure until abandonment reservoir pressure (Very Low Reservoir Abandonment Pressure)

Both the IGIP by field and by wells in Decline Curve Method show the differences due to subjectivity in the techniques to plot the decline by field & well by well. It can also show there if there is still opportunity to optimize the field production by reducing compressor intake pressure to the lowest until reservoir abandonment pressure reached, so well by well production can produce optimally and decline prediction will give the close number in IGIP estimation between field with total well by well.

IV.3 Drainage Area

From figure 4-11 can show each wells of “X” gas field having the same drainage area as cumulative production till January 2014 where gas cumulative production each wells of Mdl-01 is 16.4 BSCF, Mdl-02 is 16.2 BSCF and Mdl-03 is 16.7 BSCF.. It is caused that the reservoir characteristic in “X” gas field area is homogeneous both fluid and rock properties and has the same characteristic as tank reservoir. As geologically assessment that shows no compartmentalization issues found. By comparing the IGIP by well and by field, it looks the current existing wells will drainage the gas optimally as shown in table 4-1 where the reserve both by wells and by field have shown the close result number from material balance and decline curve methods.

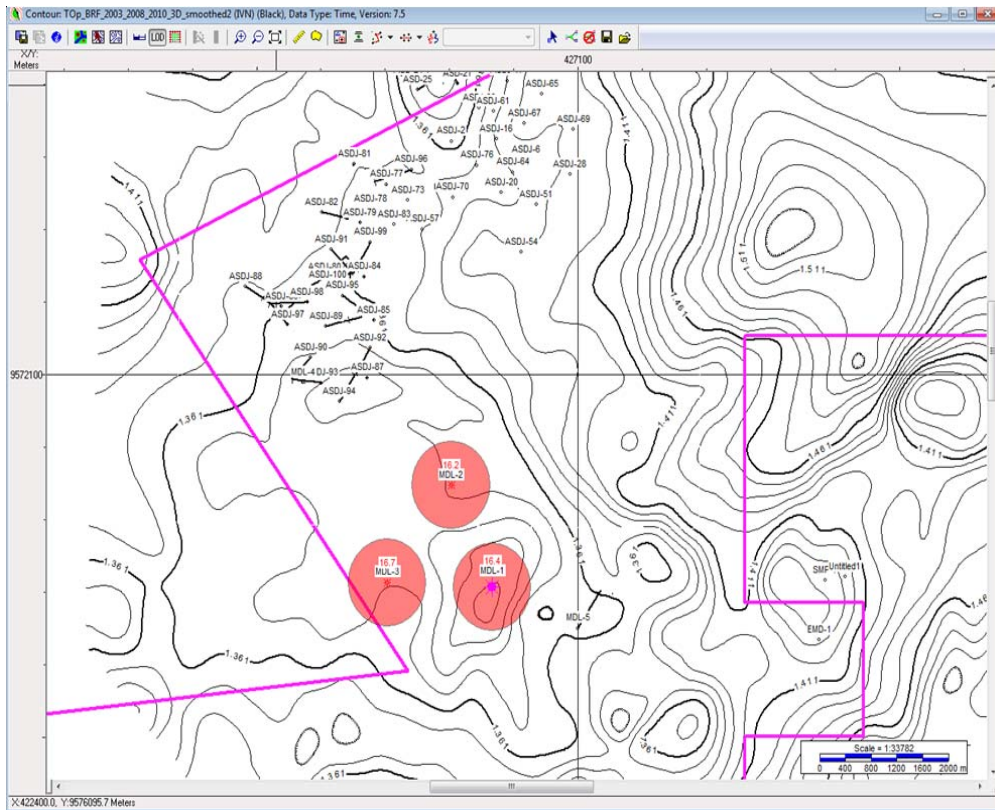


Figure 4-11 Drainage area of “X” gas field in time structure map

Meanwhile the current production rate of each wells as January 2014 as follow; Mdl-01 is 3.32 MMSCFD, Mdl-02 is 2.45 MMSCFD and Mdl-03 is 1.75 MMSCFD. Mdl-03 has the lowest gas production rate that is caused after well service in changing the tubing pump, the production has instability due to some liquid problem in wellbore. So refer to material balance and decline curve method on IGIP & EUR by wells, there will be no additional infill well development is needed since current existing 3 wells will drainage the reserve optimally until economic limit both wells and field are reached.

IV.4 Production Optimization & Surface Facility Capability

IV.4.1 Well & Field Production Deliverability & Optimization

Reviewing the production history by wells and by field at “X” gas field, it has declined from maximum about 18.6 MMSCFD in 2005 to 8-9 BSCF recently although the wells have been produced optimally as each wells can flow with maximum capacity without choke. Lowering compressor staging were done 2 times in early January 2010 and in mid of 2012 had a little production improvement in early 2010, but gave significant impact of increasing gas rate in mid of 2012 from about 5 MMSCFD to about 10.6 MMSCFD. Increasing gas production are contributed from Mdl-01 by producing from about 2 MMSCFD to about 4.7 MMSCFD and Mdl-02 from about 2 MMSCFD to about 4.4 MMSCFD meanwhile there is no significant increasing production from Mdl-03.

Evaluation of wells optimization only give the recommendation to lowering down the compressor suction pressure as low as possible to 50 psia to get very low reservoir abandonment pressure, since there is no reservoir damage observed at each wells and all of Baturaja (BRF) formations were tested and no more other formation potential from BRF 1000, BRF 1, BRF 2 and BRF 3. It is still contributed from BRF 3 and BRF 2 only few before wet and closed. The others are wet already. Another formation as Talang Akar (TAF) sands are not tested yet since the current gas sale contract can fulfill the agreement that is being produced from BRF limestone. The current existing wells are only planned for well service tubing changing due to corrosion if needed and always be monitored.

Refer to material balance model and actual data pressure lost from reservoir to slug catcher before compressor suction pressure about 170 psia, lowering suction pressure to 50 psia will give the reservoir abandonment pressure about 220 psia in reservoir. This pressure lost data is calculated by conventional technique from pressure lost from reservoir depth plus well head pressure (WHP) data and plus pressure lost from WHP to slug catcher pressure data. The lowering compressor intake pressure to 50 psia will contribute additional reserve about 6 % of IGIP from 85 % RF to 91 % or 72 BSCF to 73.6 BSCF.

IV.4.2 Surface Facility Capability

To support the field optimization by lowering compressor suction pressure until very low reservoir abandonment pressure, wells and surface facility have been accessed as explanation below. This purpose is to anticipate if any high production that will probably need facility re-construction. Wells and surface facility map of “X” gas field is shown in attachment 20.

IV.4.2.1 Pipeline & manifold

6" flowlines are interconnected wells at Mdl-01, Mdl-02 and Mdl-03 and the “X” gas field test facility from manifold to test facility with distance about 8900 m meanwhile from each wells to manifold is connected by 4" flowline with distance from 350 m till 2689 m. Approximately up to 20 MMSCFD of gas is collected from the three “X” gas field area. Any one of the three wells, or any combination of the three well flows can produce the required total flow of 20 MMSCFD. Flowlines are fusion bond epoxy (FBE) coated.

Two phase flow from three gas wells enters the inlet manifold. At any time, flow from any one well can be directed into the test header, and then into the test separator. The remaining gas and liquid flows into the group header, and from there directly to the outlet gathering line. Two phase flow from the selected ‘test’ flowline enters the test separator where it is separated into gas, hydrocarbon liquid and water phases.

Since the initial put on production of those 3 wells never reached less than 20 MMSCFD while currently the total production of “X” gas field has dropped gradually, so the existing surface facility of flow line and manifold can still

accommodate the maximum of “X” gas field production. 2 times lowering suction pressure of compressor in 2010 and 2012 with increasing gas production in 2012 is still under 11 MMSCF therefore current flowline & manifold are still able to accommodate the maximum production from now & future plan of “X” gas field production.

IV.4.2.2 Slug Catcher And Gas Liquid Separator

Gas from “X” gas field arrives at the Central Gas Facility via NPS 6 pipeline with very small liquid slugs. In addition, the NPS 6 pipeline is routinely pigged to remove any liquid remaining in the pipeline. The inlet slug catcher is designed for three phase separation: gas, free hydrocarbon liquid, and water separation, and to handle the incoming liquid slugs. A slug catcher capacity of no less than 20 bbls is provided in the vessel free board (viz. the volume between the normal and high level alarm marks).

Table 4-2 Gas liquid separator design basis

Design Throughput	5 MMSCFD Min. 15 MMSCFD Max.
Liquids flowrate	7.0 bbl/MMSCFD water, plus free hydroca liquids
Design pressure	1440 psia
Design temperature	150 °F
Corrosion allowance	0.0625 in
Manway	18 in I.D.min
Outlet liquid nozzle	internal siphon type
Corrosion test plugs	required c/w hub flange
Internal coating	Sigma 5435 epoxy or equal.

The test separator is provided with a gas outlet meter, a Daniels Senior meter to AGA report No. 3 Standards, and a positive displacement liquid flowmeter. Liquid flows out of the vessel under level control. All vessel connections are flanged. The test separator has vane pack internals. A corrosion allowance of 0.0625 inches applies to all piping and equipment exposed to CO2 containing fluids. Since the current gas production of “X” gas field has declined

and never reached up to 15 MMSCFD, so lowering suction compressor to 50 psia plan with max gas production are still able to be handled by existing slug catcher & gas liquid separator which have capacity until 15 MMSCFD.

IV.4.2.3 Compressor

“X” gas field compressor is designed for 110 % of the remainder of the gas over and above 20.0 MMSCFD necessary to achieve the total throughput, or 15.0 MMSCFD, whichever is greater from 2 compressor installed in January 2010. Below is the specification of those 2 compressors.

Table 4-3 Compressor specification with suction pressure 550 psia

Compressor design outlet temperature	125 °F
With ambient design temperature	100 °F
Suction pressure for associated gas compressors	44.7 psia. at skid edge
Suction pressure for Mandala compressor	550.0 psia. at skid edge
Discharge pressure for all compressors, normal design	964.7 psia at skid edge
Discharge pressure, maximum	1114.7 psia at skid edge
Sales gas pressure at Beringin Delivery Point	814.7 psia at flanges

In mid of 2012, lowering suction pressure to 200 psia which can design the gas flows up to 10 MMSCFD. Based on testing report, it is specified as below.

Table 4-4 Compressor specification with suction pressure 200 psia

Project name	“X” gas field compressor rental
Package name	DPC-2802 reciprocating compressor
Serial No	85889
Suction pressure / temp.	200-400 psig@130 – 160 °F
Discharge pressure / temp.	900 psig@ 130 - 160 °F
Flowrate	8.5 - 10 MMSCFD
Gas specific gravity	0.772

In this 2014, there will be proposed a project to lowering 2 suction pressure of compressors “X” gas field to 50 psia to optimize the additional reserve. The discharge pressure design will be 900 psig, and the design flow rate will be about 6 MMSCFD only.

CHAPTER V CONCLUSION AND FUTURE WORK

V.1 Conclusion

By completing the study, there are couple conclusions which can be summarized as below:

1. “X” gas field can be categorized as mature field with current recovery factor is about 60.8%
2. Refer to PVT analysis laboratory test and production history, “X” gas field is considered as a dry gas reservoir where the model from Material Balance also shows purely fluid expansion as main drive mechanism & a little bit reservoir rock expansion as drive mechanism.
3. Good history matching in Material balance model both reservoir pressure and production data gives the good IGIP estimation.
4. Refer to the combination result study of reservoir characterization and material balance model that show the close result in IGIP estimation, “X” gas field is considered as 1 reservoir tank, no compartmentalization and no aquifer support.
5. IGIP estimated from MBE shows the closed number with static and dynamic simulation from other study that is about 81 BSCF with less than 1% discrepancy, meanwhile DC analysis show lower result about 67.4 BSCF (18% discrepancy) caused by current production method is not optimally yet with compressor intake pressure is still 200 psia and limited number of economic / final flow rate which can't reach 0.
6. The current wells at “X” gas field have produced optimally with current existing completion where those 3 wells Mdl-01, Mdl-02 and Mdl-03 have produced about 16 BSCF each wells
7. Lowering the intake suction pressure of compressor was done 2 times previously, but in the second time mid of 2012 by lowering intake pressure to 200 psia has showed increasing the gas rate production from 5 MMSCFD to 10 MMSCFD. It is contributed from Mdl-01 and Mdl-02.
8. Mdl-03 well has showed no increasing gas rate production & the lowest production about 1.75 MMSCFD after lowering intake compressor

pressure to 200 psia, just sustain the production meanwhile from MBE this well gives the highest IGIP estimation based on MBE by well. Close monitoring and take reservoir pressure data routinely is highly recommended to evaluate more detail and get the precise result since the IGIP estimation shows the greatest value meanwhile the current production show the lowest result compared with 2 other wells, Mdl-01 & Mdl-02.

9. Since those 3 wells at “X” gas field can produce optimally and contribute the close number of cumulative gas production each wells up to date, no infill wells are needed. The total IGIP estimation by wells can cover IGIP by field, so current existing wells can drainage the reserve optimally until reservoir abandonment pressure reached to the lowest about 220 psia.
10. Lowering compressor suction pressure to 50 psia will give the reservoir abandonment pressure about 220 psia which can give additional reserve 6% of IGIP or improving RF from 82% to 91.5%.
11. Assessment to existing wells and facility at “X” gas field indicates current existing facilities can handle the production although the compressor intake pressure will be reduced to 50 psia since the 2 compressors will only give maximum output about 6 MMSCFD.

V.2 Future Work

There are some plans must be done for future work as follow:

1. Take the reservoir pressure data at Mdl-03 wells since the well show the discrepancy IGIP by wells between MBE and DC where IGIP from MBE shows the big number compared with DC.
2. Continuing compressor design to be lowered to 50 psia and schedule good plan without giving the production disturbance since there are 2 compressor and 3 wells that deals with this activity.
3. Opportunity to study for reducing pressure lost from reservoir to compressor

REFERENCES

- Ahmed, T. (2006). *"Reservoir Engineering Handbook"*. Oxford: Gulf Professional Publishing.
- James F. Lea, H. V. (2008). *"Gas Well Deliquification"*. Oxford: Gulf Professional Publishing.
- McCain, W. D. (1990). *"The Properties of Petroleum Fluids"*. Tulsa, Oklahoma: PenWell Books.
- McCain, W. D. (1994). Heavy Components Control Reservoir Fluid Behaviour. *Journal Petroleum Technology*, 746-750.
- Smith, R. (1990). *"Practical Natural Gas Engineering"*. Tulsa, Oklahoma: PennWell Books.
- Talisman, J. P. (2007). *"Mandala Gas Study Report"*. Jakarta: JOB Pertamina Talisman.

Attachment 1 PVT study of samples from the MDL-1

Component	Separator	Separator Gas		Well Stream	
	Liquid Mol%	Mol%	GPM	Mol%	GPM
Hydrogen Sulfide	0	0		0	
Carbon Dioxide	3.71	8.39		8.35	
Nitrogen	0.26	2.87		2.85	
Methane	19.11	81.68		81.11	
Ethane	2.66	3.04	0.812	3.04	0.813
Propane	4.98	2.1	0.577	2.13	0.587
Iso-Butane	1.49	0.31	0.102	0.32	0.105
N-Butane	3.16	0.5	0.157	0.52	0.164
Iso-Pentane	2.52	0.23	0.085	0.25	0.091
N-Pentane	2.49	0.19	0.068	0.21	0.076
Hexanes	6.1	0.22	0.09	0.27	0.105
Heptanes	13.65	0.26	0.096	0.38	0.16
Octanes	17.57	0.15	0.068	0.31	0.141
Nonanes	9.71	0.04	0.019	0.13	0.065
Decanes	5.88	0.01	0.008	0.06	0.033
Undecanes	3.07	0.01	0.004	0.04	0.024
Dodecanes	1.54	0	0	0.02	0.013
Tridecanes	0.9	0	0	0.01	0.007
Tetradecanes	0.53	0	0	0	0
Pentadecanes	0.43	0	0	0	0
Hexadecanes	0.12	0	0	0	0
Heptadecanes	0.05	0	0	0	0
Octadecanes	0.04	0	0	0	0
Nonadecanes	0.01	0	0	0	0
Eicosanes plus	0.02	0	0	0	0
Total	100	100	2.086	100	2.384

Properties of Heptane Plus :

°API Gravity at 60°F	49.5				
Density, gm/cc	0.7818		0.737		0.7597
Molecular Weight	111.8		103		107.4

Attachment 2 PVT study of samples from the MDL-2

Component	Separator Liquid Mol%	Separator Gas		Well Stream	
		Mol%	GPM	Mol%	GPM
Hydrogen Sulfide	0	0		0	
Carbon Dioxide	3.92	9.13		9.05	
Nitrogen	0.25	2.81		2.77	
Methane	18.72	80.11		79.14	
Ethane	2.46	3.07	0.822	3.06	0.818
Propane	4.16	2.46	0.678	2.49	0.686
Iso-Butane	1.04	0.4	0.13	0.41	0.134
N-Butane	2.08	0.65	0.204	0.67	0.211
Iso-Pentane	1.76	0.25	0.092	0.27	0.099
N-Pentane	1.84	0.2	0.074	0.23	0.083
Hexanes	5.36	0.25	0.101	0.33	0.128
Heptanes	13.2	0.29	0.11	0.49	0.206
Octanes	18.61	0.17	0.071	0.46	0.209
Nonanes	11.08	0.04	0.021	0.22	0.11
Decanes	7.01	0.02	0.011	0.13	0.071
Undecanes	3.79	0.03	0.017	0.09	0.053
Dodecanes	1.98	0.05	0.029	0.08	0.051
Tridecanes	1.15	0.05	0.035	0.07	0.048
Tetradecanes	0.7	0.02	0.018	0.03	0.022
Pentadecanes	0.57	0	0	0.01	0.008
Hexadecanes	0.16	0	0	0	0
Heptadecanes	0.1	0	0	0	0
Octadecanes	0.01	0	0	0	0
Nonadecanes	0.02	0	0	0	0
Eicosanes plus	0.03	0	0	0	0
Total	100	100	2.086	100	2.384

Properties of Heptane Plus :

°API Gravity at 60°F	49.1				
Density, gm/cc	0.7837		0.737		0.7647
Molecular Weight	114		103		109.4

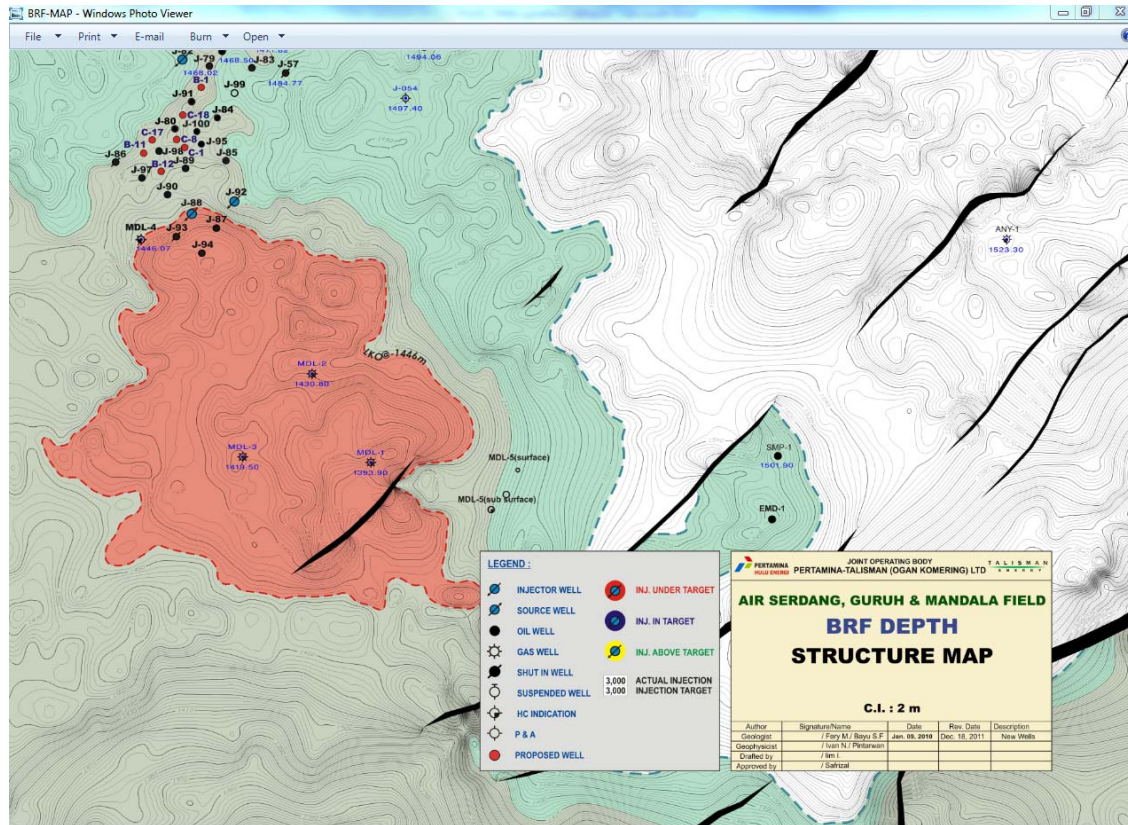
Attachment 3 PVT study of samples from the MDL-3

Component	Separator	Separator Gas		Well Stream	
	Liquid Mol%	Mol%	GPM	Mol%	GPM
Hydrogen Sulfide	0	0		0	
Carbon Dioxide	4.4	9.51		9.49	
Nitrogen	0.23	2.8		2.79	
Methane	19.05	79.77		79.49	
Ethane	2.69	2.96	0.791	2.96	0.792
Propane	5.03	2.41	0.663	2.42	0.667
Iso-Butane	1.49	0.4	0.132	0.4	0.131
N-Butane	3.19	0.66	0.208	0.67	0.211
Iso-Pentane	2.44	0.29	0.104	0.3	0.11
N-Pentane	2.43	0.24	0.086	0.25	0.091
Hexanes	5.99	0.32	0.13	0.35	0.136
Heptanes	13.41	0.38	0.147	0.44	0.185
Octanes	17.14	0.21	0.089	0.29	0.132
Nonanes	9.6	0.03	0.02	0.07	0.035
Decanes	5.83	0.01	0.007	0.04	0.022
Undecanes	3.01	0.01	0.004	0.02	0.012
Dodecanes	1.55	0	0	0.02	0.013
Tridecanes	0.99	0	0	0	0
Tetradecanes	0.74	0	0	0	0
Pentadecanes	0.43	0	0	0	0
Hexadecanes	0.17	0	0	0	0
Heptadecanes	0.08	0	0	0	0
Octadecanes	0.06	0	0	0	0
Nonadecanes	0.02	0	0	0	0
Eicosanes plus	0.03	0	0	0	0
Total	100	100	2.086	100	2.384

Properties of Heptane Plus :

°API Gravity at 60°F	49.5			
Density, gm/cc	0.7816		0.737	0.7493
Molecular Weight	112.8		103	105.6

Attachment 4 "X" gas field BRF structure map



Attachment 5 Permeability and porosity data at corresponding depths

Sample Number	Depth m	Permeability			Porosity		Saturation		Grain	Description
		(Horizontal)	(90 Deg)	(Vertical)	(Helium)	(Fluids)	(Pore Volume)		Density	
		Kair md	Kair md	Kair md			Oil %	Water %	gm/cc	
101	1510.68	0.08	-	0.05	8.7	7.4	2.1	76.6	2.72	Ls gry vf xln hd vug abd foss
102	1511.07	5.10	-	0.31	22.0	19.8	0.7	69.1	2.71	Ls gry vf xln hd tr foss carb
103	1511.60	0.18	-	0.01	6.5	8.7	1.7	57.3	2.72	Ls gry vf xln hd foss vug
104	1512.04	0.01	-	<.01	2.9	4.4	0.0	60.9	2.72	Ls gry vf xln hd foss
105	1512.54	21.00	-	0.13	16.1	12.4	0.0	60.9	2.72	Ls gry vf xln hd foss vug
106	1513.15	1.05	-	0.39	6.5	8.8	0.9	58.1	2.71	Ls gry vf xln hd abd foss
107	1513.55	72.00	-	36.00	21.8	20.0	9.2	50.8	2.71	Ls gry vf xln hd foss vug
108	1514.00	-	-	-	-	5.2	1.5	50.5	-	Ls gry vf xln hd foss
109	1514.60	0.01	-	0.01	2.5	6.6	1.5	62.7	2.71	Ls gry vf-f xln hd foss sli vug
110	1515.04	<.01	-	<.01	4.4	-	-	-	2.71	Ls gry vf xln hd foss tr carb
111	1516.05	<.01	-	0.01	4.1	-	-	-	2.72	Ls gry vf xln hd foss
112	1517.07	0.05	-	0.01	8.7	-	-	-	2.71	Ls gry vf xln hd foss sli vug sli styl
113	1518.06	0.01	-	0.01	4.5	-	-	-	2.71	Ls gry vf xln hd tr foss sli styl
114	1519.25	0.04	-	0.03	6.9	6.1	2.5	60.5	2.72	Ls gry vf xln hd foss tr carb
115	1519.56	0.04	-	0.06	8.2	6.6	1.2	54.3	2.72	Ls gry vf xln hd foss carb lam

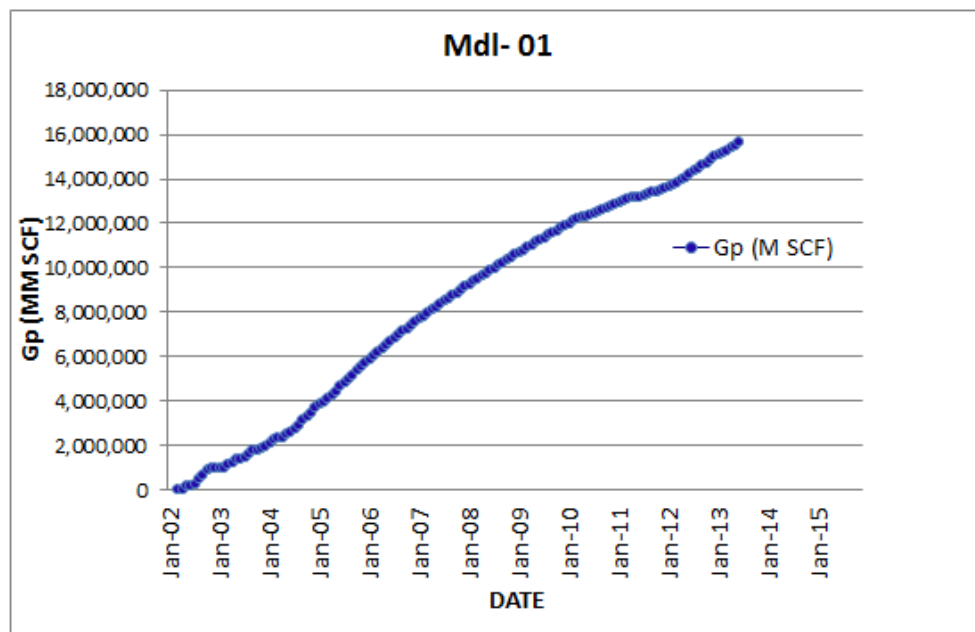
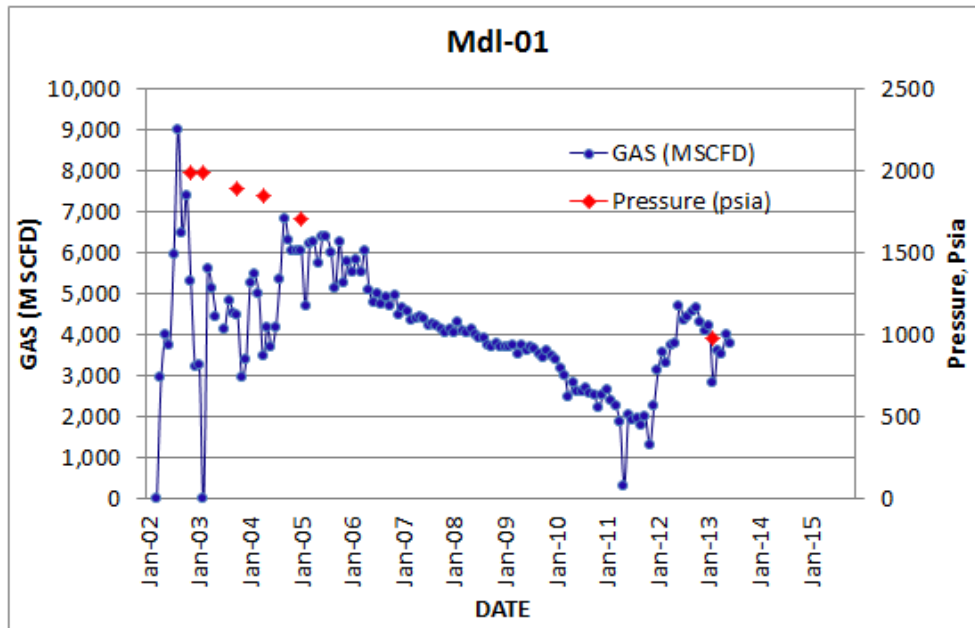
Attachment 6 Summary of log interpretation result

Well	Zone	Depth Zone		Thickness		NTG	Avg. Por %	Avg. Sw %
		Top md	Bottom md	Gross m	Net m			
MDL-1	BRF-003	1450.0	1463.5	13.50	3.75	0.28	8.08	69.06
	BRF-002	1463.5	1485.0	21.50	9.50	0.44	12.46	51.45
	BRF-001	1485.0	1505.0	20.00	9.75	0.49	8.07	91.83
	BRF-100	1505.0	1531.0	26.00	9.25	0.36	6.93	97.96
MDL-2	BRF-003	1507.5	1518.0	10.50	5.63	0.54	13.43	54.52
	BRF-002	1518.0	1538.5	20.50	10.25	0.50	11.14	81.18
	BRF-001	1538.5	1560.0	21.50	4.63	0.22	7.82	94.53
	BRF-100	1560.0	1584.0	24.00	5.63	0.23	7.79	99.36
MDL-3	BRF-003	1493.0	1505.0	12.00	10.88	0.91	12.69	45.53
	BRF-002	1505.0	1522.0	17.00	12.13	0.71	10.47	69.90
	BRF-001	1522.0	1540.0	18.00	11.75	0.65	7.80	91.90
	BRF-100	1540.0	1566.0	26.00	8.13	0.31	8.05	97.99
MDL-4	BRF-003	1508.0	1515.5	7.50	3.63	0.48	11.15	97.46
	BRF-002	1515.5	1538.0	22.50	14.13	0.63	11.76	65.64
	BRF-001	1538.0	1552.5	14.50	1.00	0.07	5.40	100.00
	BRF-100	1552.5	1573.0	20.50	4.50	0.22	7.22	100.00

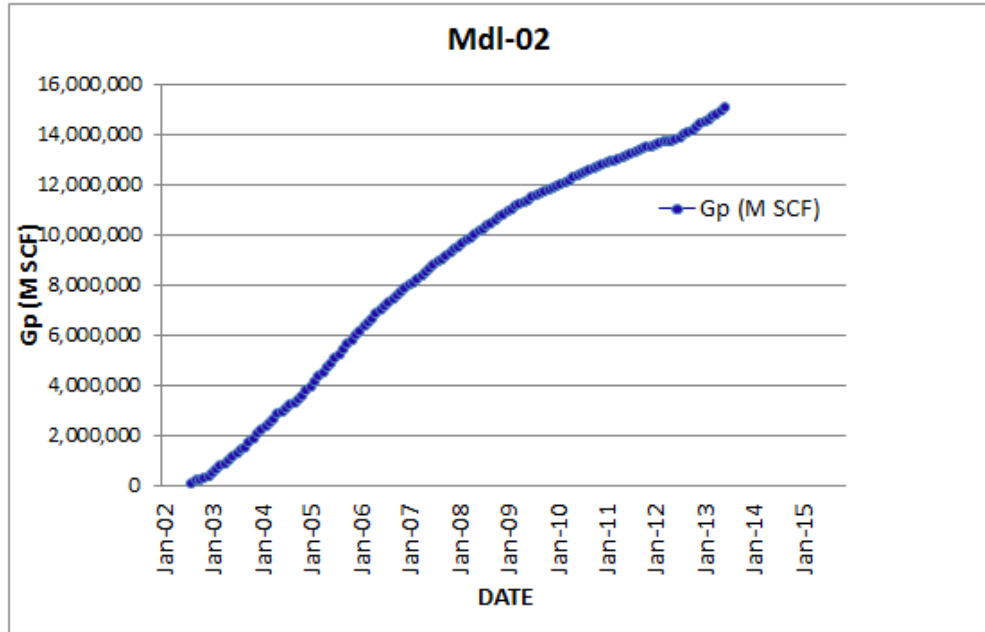
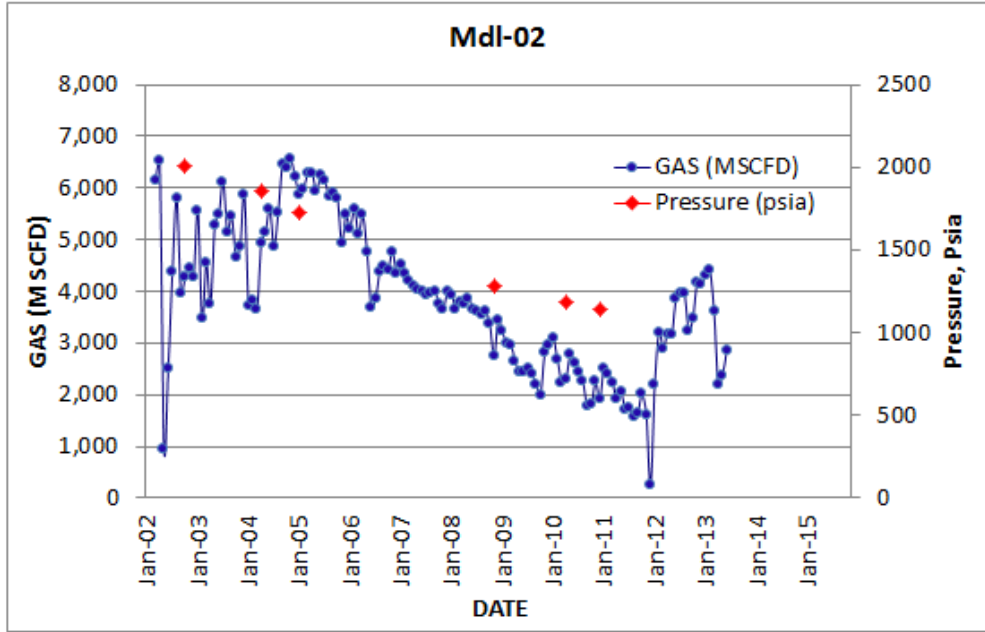
Attachment 7 "X" gas field pressure history record

WELL	DATE	ZONE	PERF INTERVAL (m MD)	KB (m)	GAUGE DEPTH		TEMP. (degF)	FINAL PRESS. (psi)	PRESS. GRAD. (psi/ft)	DATUM PRESS. (psi)	DATUM PRESS. @ 1528 MS	FLOW. PRESS. (psi)	TYPE OF SURVEY	REMARKS
					(m MD)	(MSS)								
MDL-01	7-Nov-02	BRF	1450-1473.5	56.5	1,449.5	1,393	223.7	1,982	0.030	1,987	1,995		DST-7B	gas
	28-Feb-03	BRF	1450-1473.5	56.5	1,430.0	1,374	225.9	1,981	0.030	1,988	1,997		DST-8A	gas
	17-Oct-03	BRF	1450-1473.6	56.5	1,430.0	1,374	227.0	1,883	0.030	1,890	1,898		DST-9A	gas
	7-Apr-04	BRF	1450-1473.7	56.5	1,430.0	1,374	228.3	1,835	0.030	1,842	1,850		DST-10A	
	30-Jan-05	BRF	1450-1473.8	56.5	1,425.0	1,369	227.0	1,695	0.030	1,703	1,711		DST-7B	
	28-Feb-13	BRF	1450-1473.5	56.5	1,430.0	1,374	224.9	975	0.023	981	987		BHP	gas
MDL-02	20-Oct-02	BRF	1507.5-1514.5	76.2	1,513.3	1,437	220.7	2,005	0.030	2,006	2,014		DST-8A	
	9-Apr-04	BRF	1507.5-1514.5	76.2	1,513.3	1,437	229.5	1,860	0.030	1,861	1,869		DST-9A	
	31-Jan-05	BRF	1507.5-1514.5	76.2	1,502.0	1,426	109.1	1,721	0.030	1,723	1,731		DST-10A	
	25-Nov-08	BRF	1507.5-1514.5	76.2	1,513.4	1,437	222.0	1,283	0.031	1,284	1,293		SG & TG	
	3-Apr-10	BRF	1507.5-1514.5	76.2	1,518.0	1,442	224.3	1,181	0.237	1,184	1,248			
	20-Dec-10	BRF	1507.5 - 1514.5	76.2	1,511.0	1,435	224.7	1,140	0.027	1,141	1,149		SG & TG	
MDL-03	21-Oct-01	BRF	1450 - 1459.5	73.5	1,435.0	1,362	206.9	2,101	0.019	2,106	2,111		DST-7B	
	11-Feb-05	BRF	1451 - 1459.5	73.5	1,467.0	1,394	227.0	1,727	0.040	1,734	1,745		DST-8A	
	17-Feb-06	BRF	1493-1504	73.5	1,464.8	1,391	226.0	1,585	0.038	1,592	1,602		DST-9A	gas
	31-Jan-07	BRF	1493-1504	73.5	1,475.8	1,402	226.0	1,463	0.034	1,468	1,477		DST-10A	gas
	1-Jun-07	BRF	1493-1504	73.5	1,498.5	1,425	227.9	1,431	0.001	1,431	1,432		DST-7B	gas
	13-Feb-08	BRF	1493-1504	73.5	1,475.8	1,402	225.3	1,361	0.040	1,366	1,377	1,196.9	SG & TG	gas
	30-Aug-09	BRF	1493-1504	73.5	1,461.4	1,388	218.7	1,222	0.035	1,229	1,238		SG & TG	
	10-Jul-11	BRF	1493-1504	73.5	1,464.8	1,391	220.4	1,121	0.091	1,138	1,162		SG & TG	

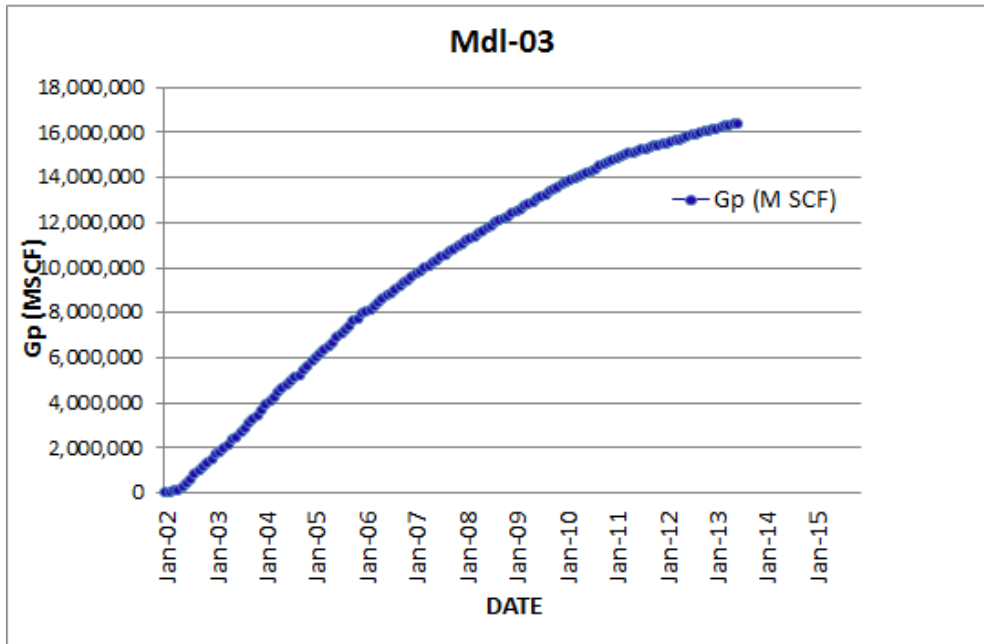
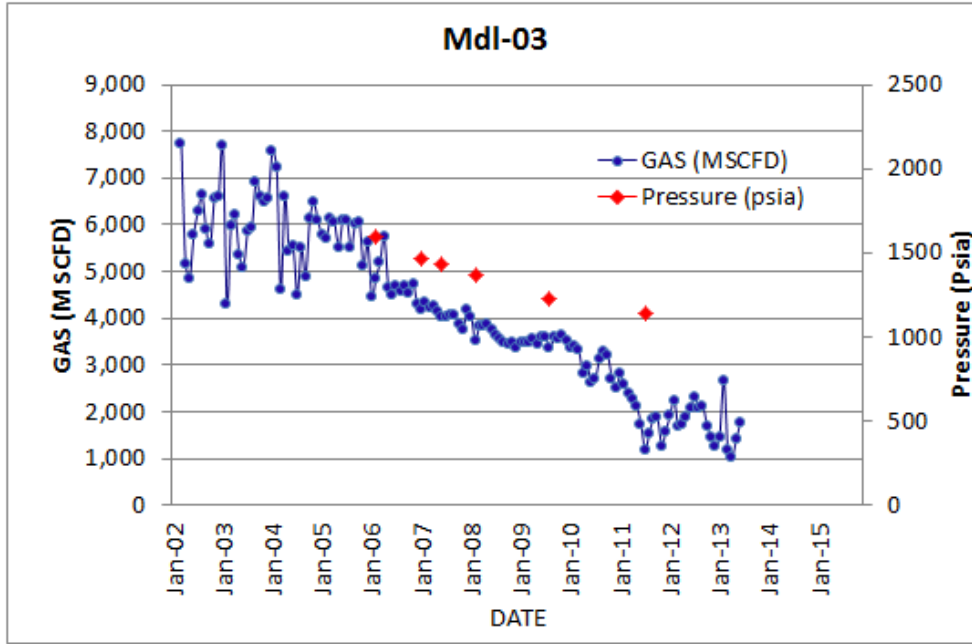
Attachment 8 Production and reservoir pressure history Mdl-01



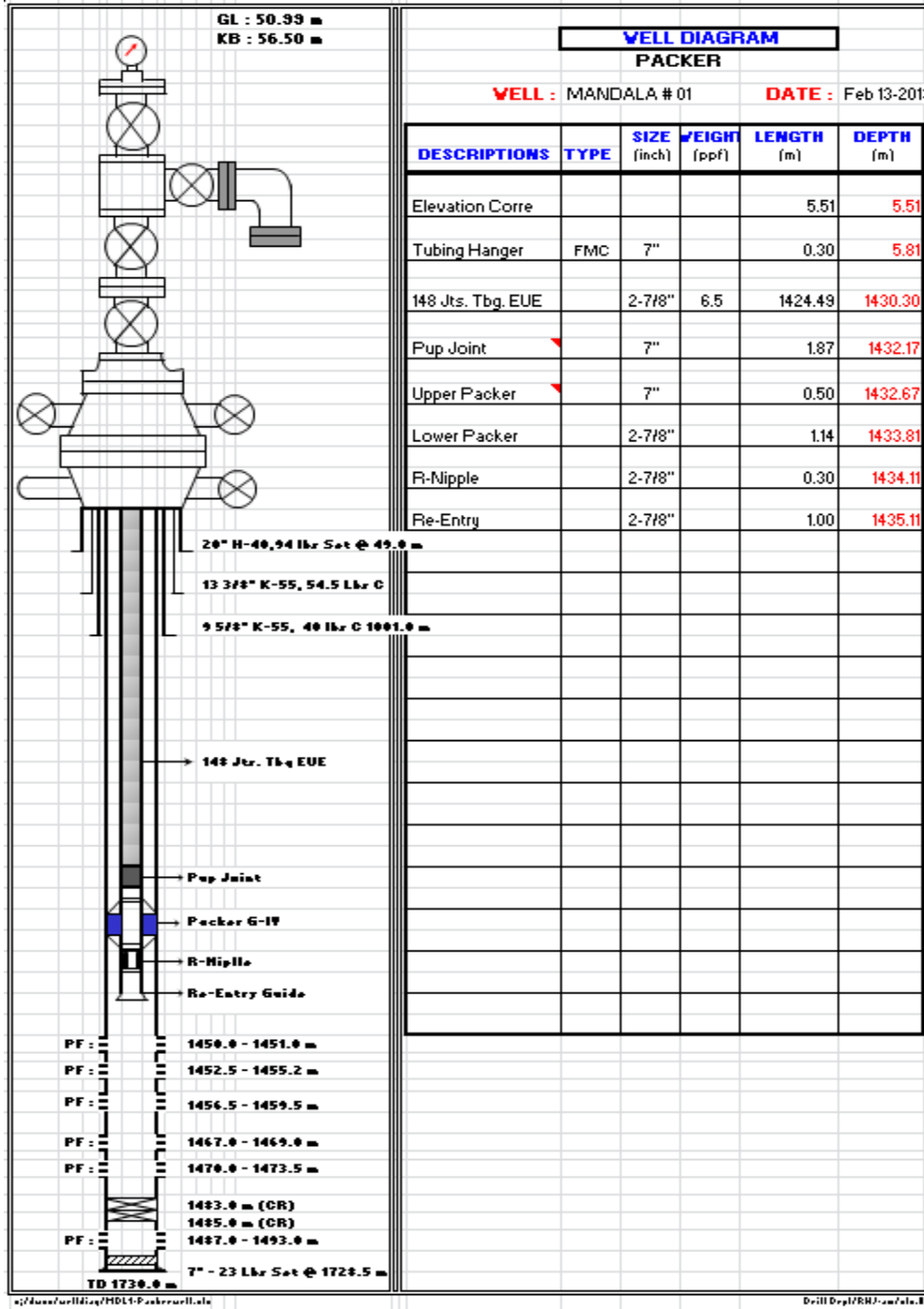
Attachment 9 Production and reservoir pressure history Mdl-02



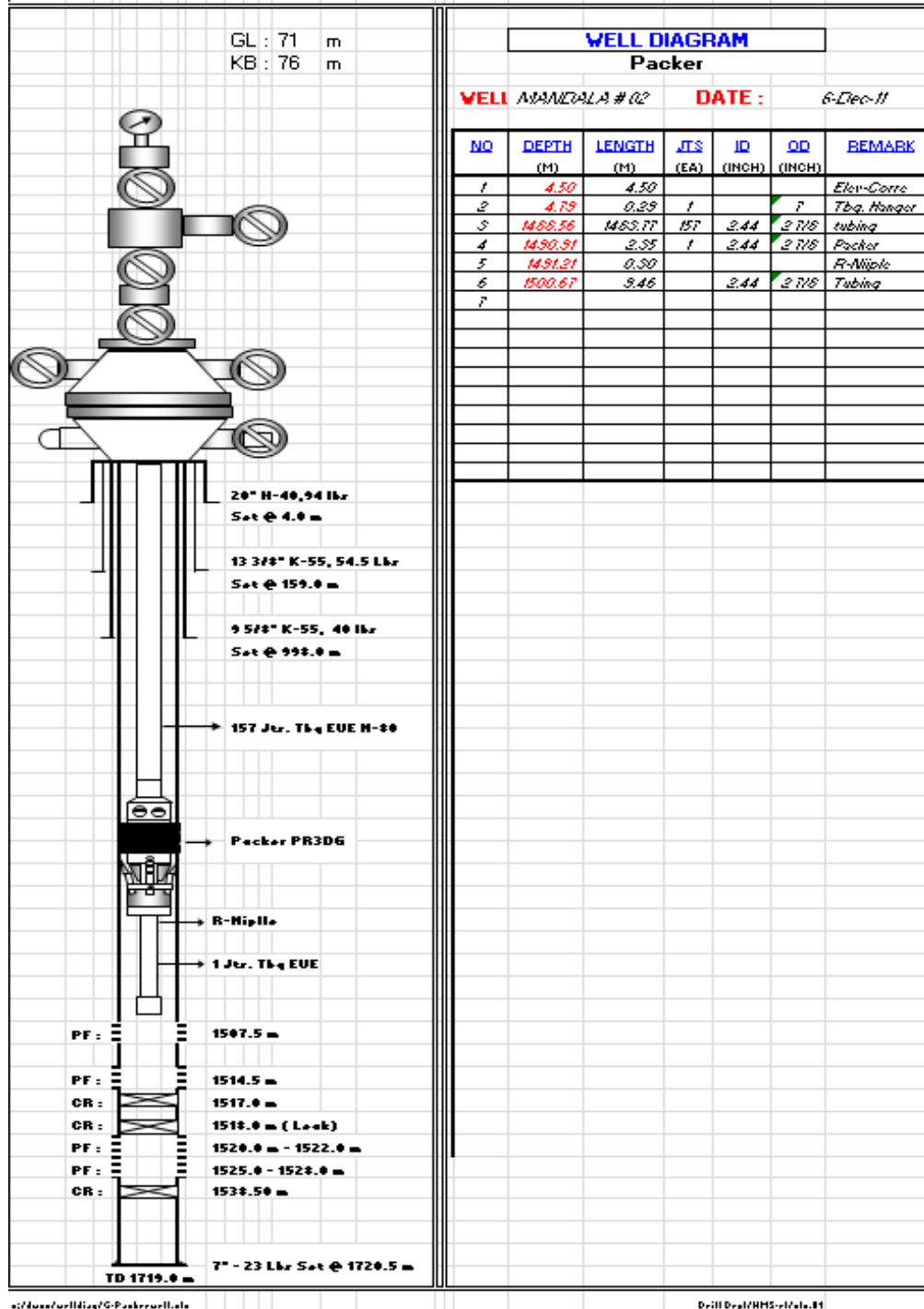
Attachment 10 Production and reservoir pressure history Mdl-03



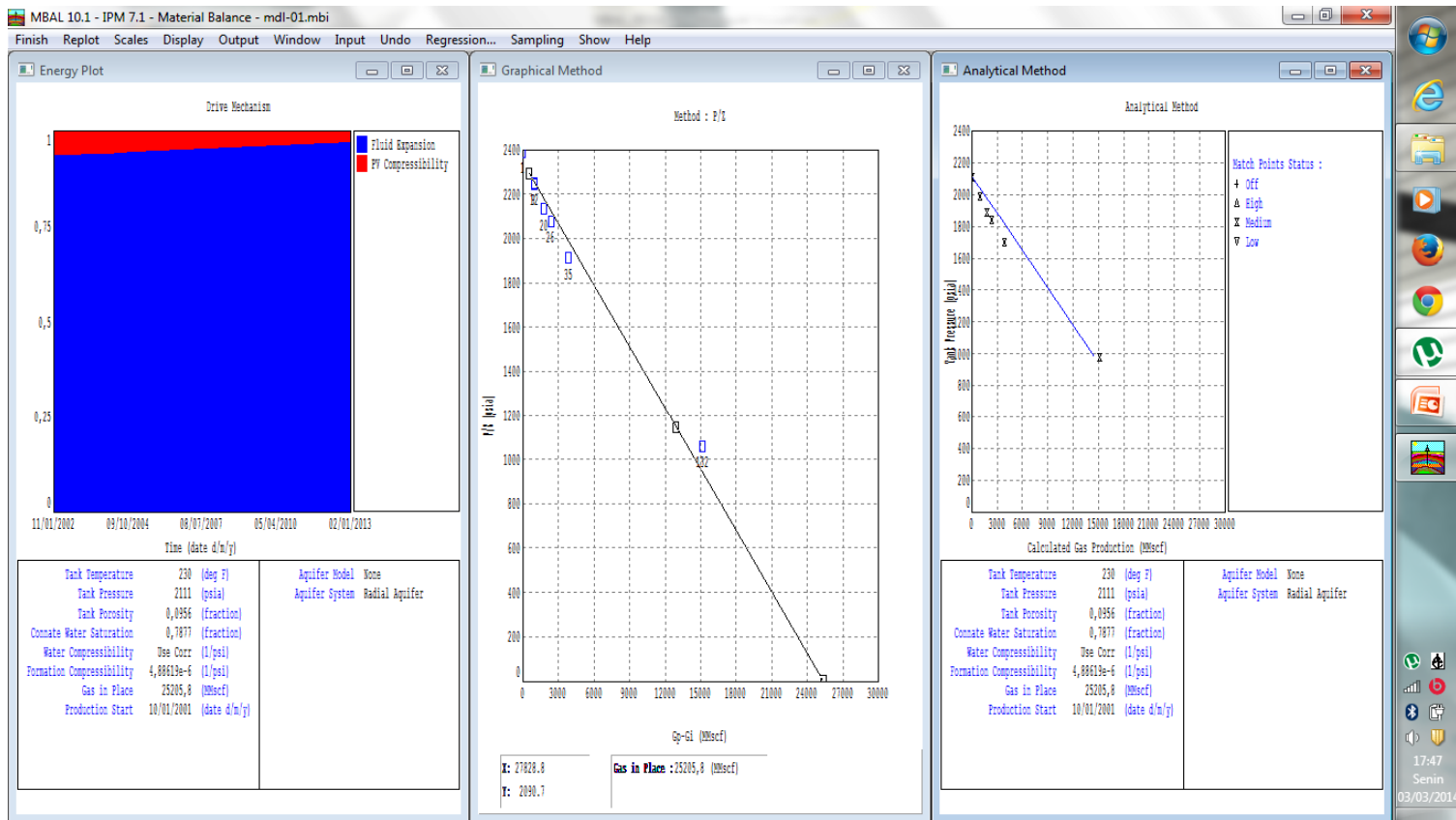
Attachment 11 Well diagram Mdl-01



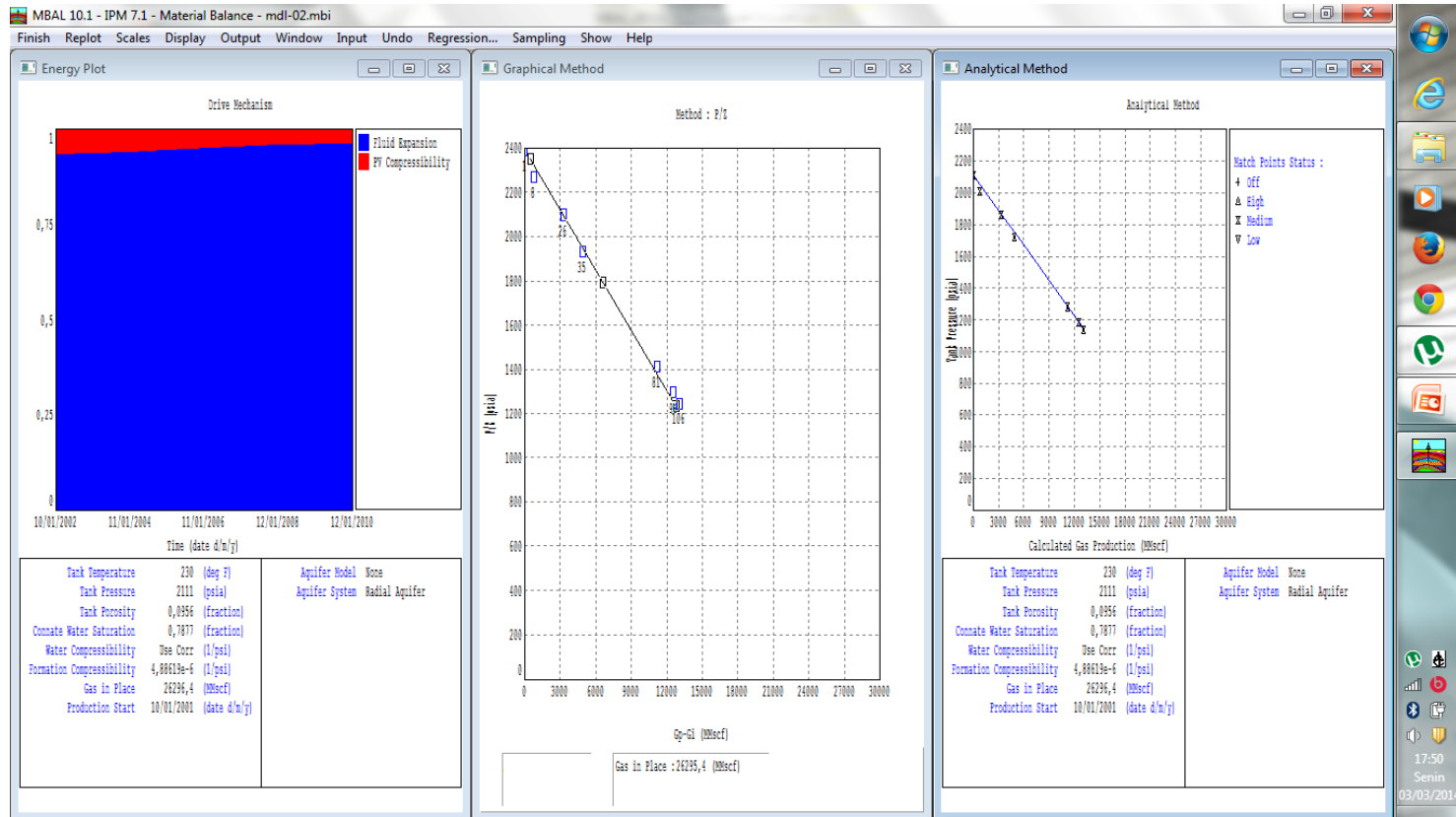
Attachment 12 Well diagram Mdl-02



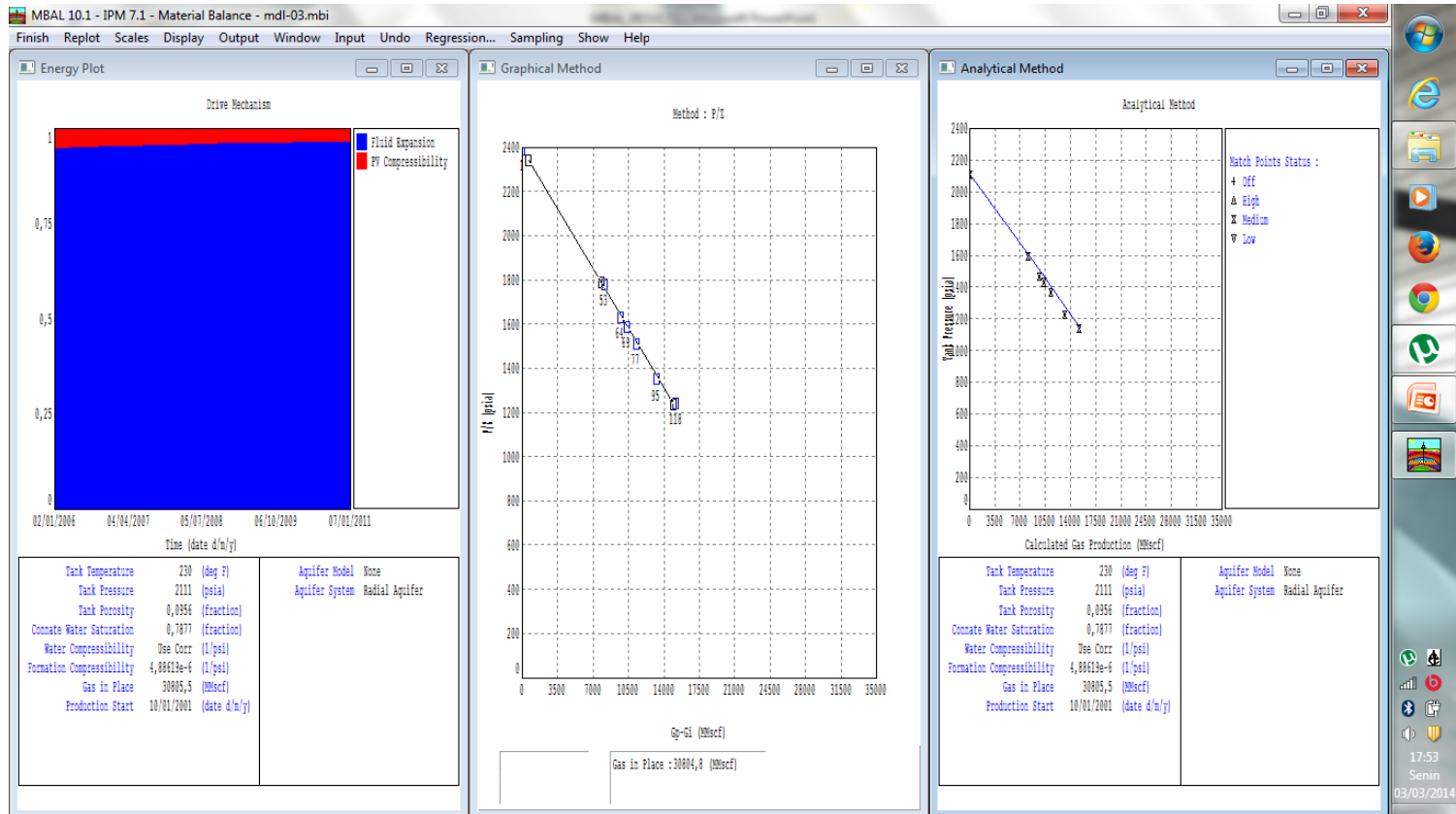
Attachment 14 IGIP Mdl-01 based on MBE model



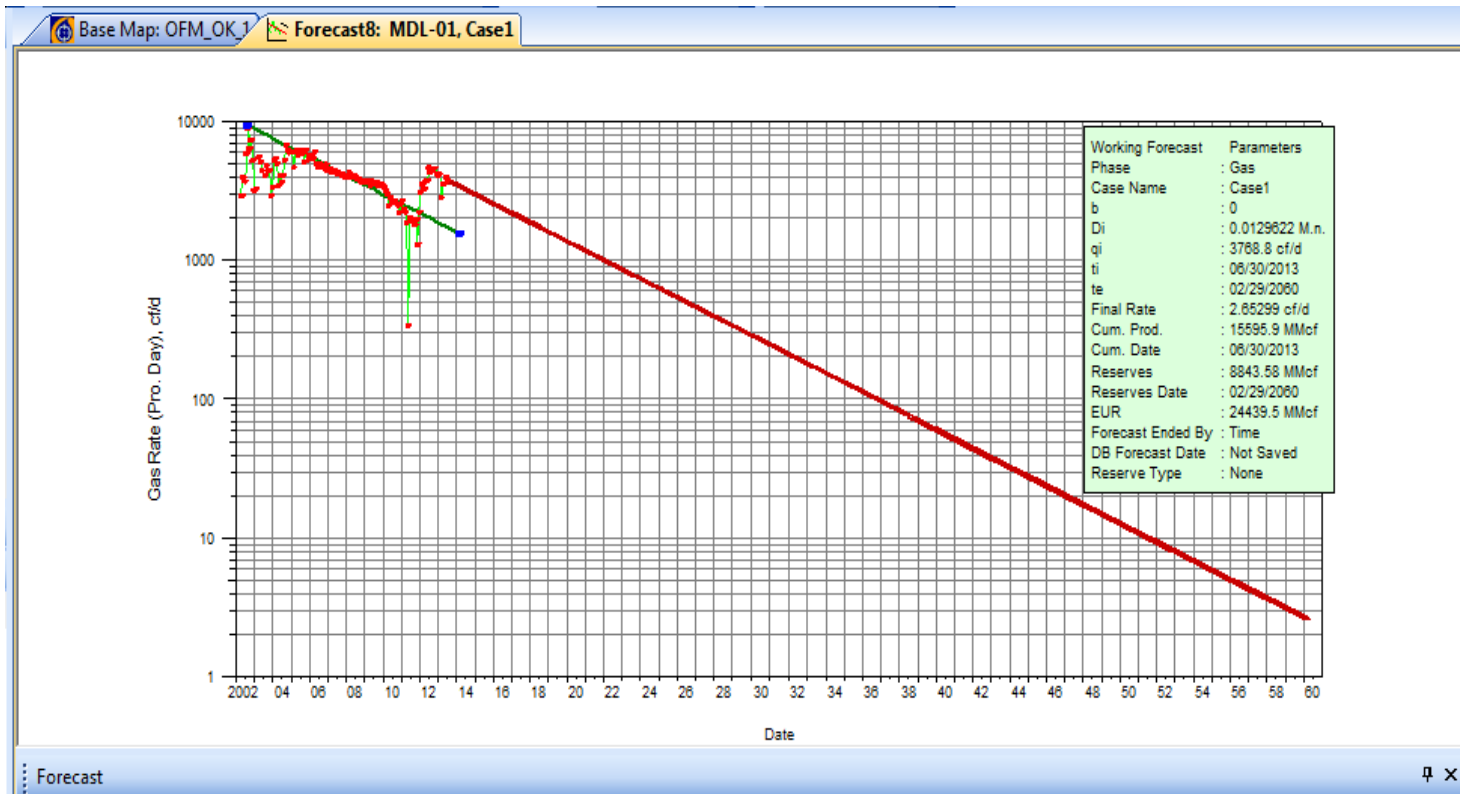
Attachment 15 IGIP Mdl-02 based on MBE model



Attachment 16 IGIP Mdl-03 based on MBE model



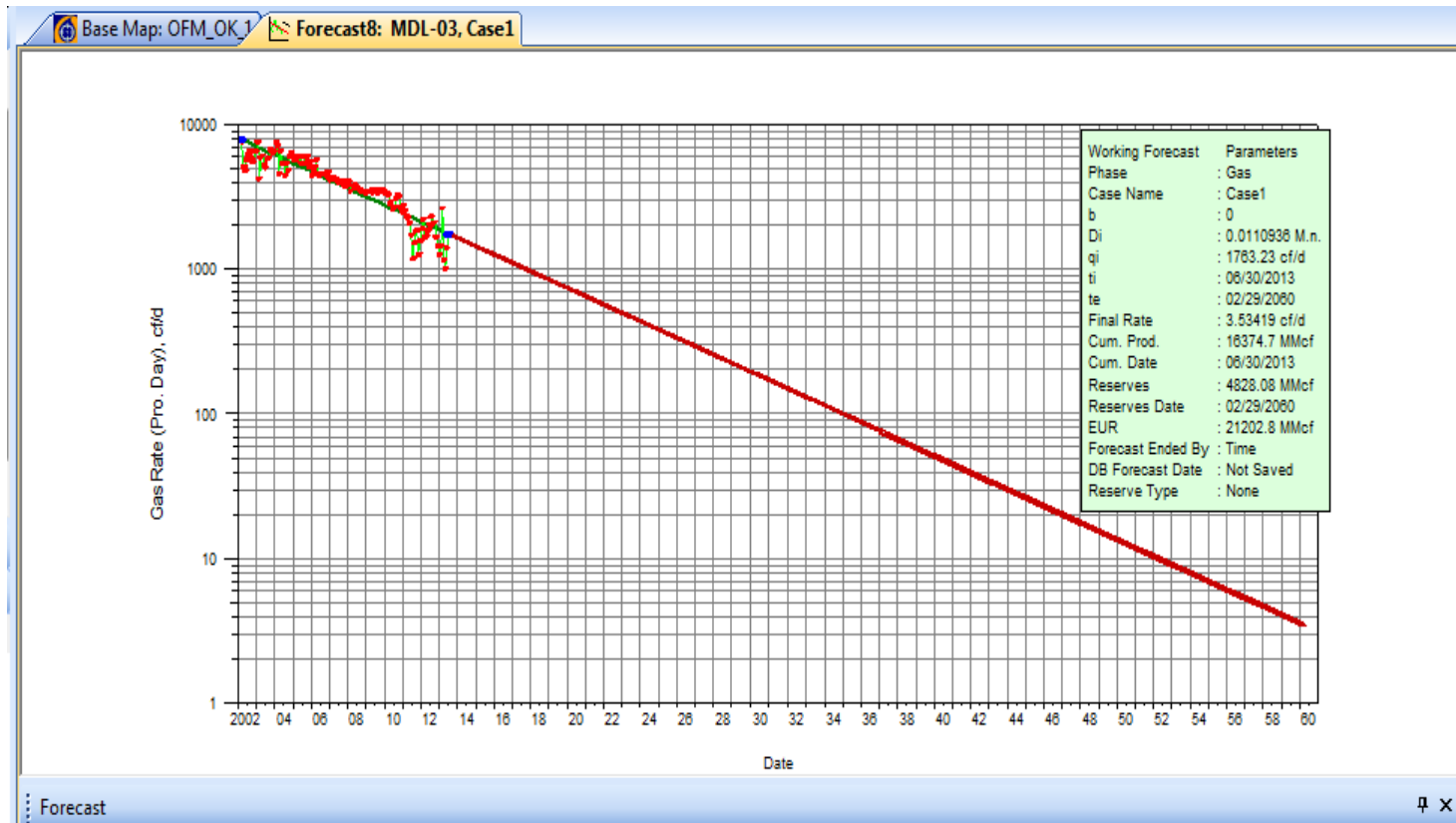
Attachment 17 IGIP Mdl-01 based on DC analysis



Attachment 18 IGIP Mdl-02 based on DC analysis



Attachment 19 IGIP Mdl-03 based on DC analysis



Attachment 20 Schematic wells and surface facilities “X” gas field

